CX3CL1/CX3CR1 Signaling Mediated Neuroglia Activation Is Implicated in the Retinal Degeneration: A Potential Therapeutic Target to Prevent Photoreceptor Death

Jie-Min Huang, Na Zhao, Xiao-Na Hao, Si-Yu Li, Dong Wei, Ning Pu, Guang-Hua Peng, and Ye Tao

Department of Physiology and Neurobiology, Laboratory of Visual Cell Differentiation and Regulation, School of Basic Medical Sciences, Zhengzhou University, Zhengzhou, China

Correspondence: Ye Tao and Guang-Hua Peng, Department of Physiology and Neurobiology, Laboratory of Visual Cell Differentiation and Regulation School of Basic Medical Sciences, Zhengzhou University, 100 Science Avenue, Zhengzhou 450001, China; panghtoyezz@zzu.edu.cn, ghp@zzu.edu.cn.

JMH and NZ contributed equally to this work.

Received: September 8, 2023
Accepted: December 17, 2023
Published: January 17, 2024

Citation: Huang JM, Zhao N, Hao XN, et al. CX3CL1/CX3CR1 signaling mediated neuroglia activation is implicated in the retinal degeneration: A potential therapeutic target to prevent photoreceptor death. *Invest Ophthalmol Vis Sci.* 2024;65(1):29. https://doi.org/10.1167/iovs.65.1.29

Purpose. Retinal degeneration (RD) is a large cluster of retinopathies that is characterized by the progressive photoreceptor death and visual impairments. CX3CL1/CX3CR1 signaling has been documented to mediate the microglia activation and gliosis reaction during neurodegeneration. We intend to verify whether the CX3CL1/CX3CR1 signaling is involved in the RD pathology.

Methods. A pharmacologically induced RD mice model was established. AZD8797, a CX3CR1 antagonist, was injected into the vitreous cavity of an RD model to modulate the neuroglia activation. Then, the experimental animals were subjected to functional, morphological, and behavioral analysis.

Results. The CX3CL1/CX3CR1 signaling mediated neuroglia activation was implicated in the photoreceptor demise of an RD model. Intravitreal injection of AZD8797 preserved the retinal structure and enhanced the photoreceptor survival through inhibiting the CX3CL1/CX3CR1 expressions. Fundus photography showed that the distribution of retinal vessel was clear, and the severity of lesions was alleviated by AZD8797. In particular, these morphological benefits could be translated into remarkable functional improvements, as evidenced by the behavioral test and electroretinogram (mf-ERG) examination. A mechanism study showed that AZD8797 mitigated the microglia activation and migration in the degenerative retinas. The Müller cell hyper-reaction and secondary gliosis response were also suppressed by AZD8797.

Conclusions. The neuroinflammation is implicated in the photoreceptor loss of RD pathology. Targeting the CX3CL1/CX3CR1 signaling may serve as an effective therapeutic strategy. Future refinements of these findings may cast light into the discovery of new medications for RD.

Keywords: neurodegeneration, oxidative stress, visual impairments, photoreceptor

The retina is a peripheral component of central nervous system that is responsible for converting visible light into neural signals.[1] It is composed of multiple layers of retinal neurons and glia cells. As the most common type of retinal neuroglial, Müller cells extend their axons across retinal layers, providing metabolic and neurotrophic support to neurons.[2–4] Microglia is another type of resident neuroglia which are constantly engaged in the surveillance of endogenous immune environment.[5] Generally, microglia cells are distributed in the inner plexiform layer (IPL) and the outer plexiform layer (OPL) with ramified shapes.[6] Once the retina is exposed to pathological insults, microglia cells are activated rapidly and form tightly connected clusters in the damaged area by moving laterally and vertically in the retina within a few hours. They phagocytose the debris of dead photoreceptor while also communicate with monocytes to accelerates the pathological process of retinal degeneration (RD).[7] The activated microglia adapt their morphology from a ramified to an amoeboid form, and migrate to the outer layer.[5,8] Amoeboid microglia respond vigorously to the stimulus through producing a cluster of inflammatory cytokines, for example, the tumor necrosis factor-α (TNF-α), interleukin-1β (IL-1β), reactive oxygen species (ROS), and reactive nitrogen species (RNS), which subsequently cause chronic inflammation in the retina.[9]

Retinal degeneration (RD) is a retinopathy that is characterized by the progressive demise of photoreceptors, vessel atrophy, and visual impairments.[10,11] As a multifactorial disease, RD evolves from complex genetic and environmental backgrounds.[12] The initiator of RD pathology can be traced to the retina pigment epithelium (RPE) cells,

which are engaged in the daily phagocytosis of photoreceptor debris and the recycle of visual pigments.[13] When the autophagy capacity of RPE cells is impaired, insufficient digested organelles will accumulate and form extracellular drusen deposits.[14,15] These drusen deposits subsequently trigger chronic inflammation and oxidative damages in the subretinal space.[16–19] Recent studies show that the dysregulation of inflammatory response may serve as a driving force behind the development of RD.[20,21] In a genetic RD animal model, the activated microglia aggregates in the subretinal space and contributes to the intensified inflammation.[22] Pervasive microglia infiltration is also detected in the subretinal space of patients with RD. In particular, the activated microglia promote retinal angiogenesis under hypoxic stress and guide immature blood vessels into unvascularized areas (such as the outer nuclear layer [ONL] and macula) through neurovascular coupling.[23] In this context, chronic neuroinflammation is intimately involved in the RD pathogenesis , but the details of the underlying mechanism remains enigmatic.[22]

CX3CL1 is a chemokine of the CX3C family that is abundantly expressed in retinal neurons, whereas its sole receptor CX3CR1 is predominantly expressed in microglia cells.[24] CX3CL1/CX3CR1 signaling enables the efficient communication between the neurons and microglia.[25] CX3CL1 is an adhesion molecule that plays an inhibitory role in the pro-inflammatory response, as they can present CX3CR1 into the microglia cells and maintain them in a quiescent state.[26] CX3CL1 are synthesized as transmembrane molecules that can be cleaved from the cell surface to produce soluble forms under pathological conditions. The soluble isoform of CX3CL1 can access the cytoplasm through binding with CX3CR1 and consequently trigger the chemotactic signaling pathways. Through modulating the activity of several proteases, CX3CL1 is able to initiate the neuroinflammation response and the progression of neurodegenerations.[27] Under pathological conditions, CX3CL1/CX3CR1 signaling has been shown to mediate the microglia activation, localization, and motility.[28] On the other hand, blocking the CX3CL1/CX3CR1 interactions by neutralizing antibodies can alleviate the microglia mediated inflammation and oxidative stress.[29] AZD8797 is an allosteric modulator of CX3CL1 which can noncompetitively bind with CX3CR1 and affect the downstream G-protein activation.[30] AZD8797 can mitigate the inflammatory response in the neural tissue through inhibiting the release of IL-1β, IL-6, and TNF-α.[31] AZD8797 can also inhibit the infiltration of leukocyte in the central nervous system (CNS).[32] However, whether the AZD8797 can affect the microglia activity in the degenerative retina remains unknown.

System administration of sodium iodate ($NaIO_3$) is a classic method to induce RD in rodents.[33] The induced pathological signs, such as disrupted ONL, atrophic pigment epithelial lesions, and impaired visual function, are similar to the clinical features of patients with RD.[34,35] Thus far, the $NaIO_3$-induced RD model has been used extensively for studying pathology and developing therapies for RD.[36] In this study, we find that the neuroglia activation is implicated in the photoreceptor death of an RD model. On the other hand, intravitreal injection of AZD8797 can enhance the photoreceptor survival and inhibit retinal inflammation through CX3CL1/CX3CR1 signaling in RD. Future refinements of these findings may provide a new therapeutic approach for degenerative retinopathy.

Methods

Animals and Drug Therapy

C57BL/6J mice (6–8 weeks, weight 20–25 g) were kept in a 20 to 25°C animal chamber which 12 hour:12 hour (8:00–20:00) circadian cycle. $NaIO_3$ (7681-55-2; Sigma, St. Louis, MO, USA) was stored at 4°C and dissolved in phosphate buffered saline (PBS) of 10 mg/kg before use. An RD mice model was established by a single intraperitoneal injection of $NaIO_3$ at a dose of 60 mg/kg. AZD8797 (HY-13848; MedChemExpress, Los Angeles, CA, USA) was dissolved in 10% DMSO (3.125 ng/µL), and then was injected into the vitreous body using a 29 G microlight syringe (Model 701; Hamilton Company, Reno, NV, USA). AZD8797 was administered through a single intravitreous injection within 2 hours post modeling. Totally, 300 mice were used in this study. In the first section, studying the pathological signs of RD model, 100 mice were used for establishing the RD model, and then they were used for pathological analysis at five time points after modeling. In the therapeutic section, animals were randomly divided into four groups: (1) normal control group ($n = 50$); (2) RD group ($n = 50$): intraperitoneal injection 60 mg/kg $NaIO_3$; (3) RD + vehicle group ($n = 50$): RD mice received an intravitreal injection of DMSO; and (4) RD + AZD8797 group ($n = 50$): RD mice received an intravitreal injection of AZD8797. The therapeutic effects were evaluated at P14 and P28 after treatment. The protocol of animal handling was in accordance with the ARVO Guidelines for ophthalmic and visual research. It was approved by the Institutional Animal Care and Use Committee of Zhengzhou University. All efforts were made to minimize the number of animals used and their suffering.

Light/Dark Box Test

The light/dark box system (TopScan; CleverSys, Inc., Reston, VA, USA) is composed of a monitoring device and two closed boxes. The surrounding environment was kept quiet to reduce possible influence on the animal. TopScan version software was used to record and analyze the animal trace within the light/dark box. The examiner set the initial background and observation scope. Mice moved freely in the light/dark box for 10 minutes, and their movements were recorded by a real-time video. The gained data were exported in the form of movement track diagram and density heat diagram.

Open Field Test

The bottom surface of the open field device (TopScan; CleverSys, Inc.) is a 40 cm × 40 cm square. TopScan version software was used to monitor the animal movements within open field box for 10 minutes. Behavioral parameters, including the total distance, speed, and time of movement in the central region of mice, were analyzed statistically on the basis of the track diagram and density heat diagram.

Optokinetic Behavioral Test

A mouse was placed on an elevated platform with a height of 14.5 cm in the middle of the OptoMotry system (Clever Sys Inc.). The OptoMotry system is made up of four LED displays on all sides and mirrors on the ceiling and floor. The stimuli form a virtual rotating raster with a black and

white stripe pattern. When the grating was projected onto the inner wall by an LED and rotates at a certain speed, the mouse will track the stimulus by turning its head. In the experiment, the motor response test is recorded automatically when the head movement score exceeds the chance level of stimulation-independent head movement provided by the OptoMotry algorithm.

Multifocal Electroretinogram

Mice were anaesthetized by intraperitoneal injection of 5% chloral hydrate (0.0008 mL/g). A compound tropicamide eye drop was used to dilate the pupils of the eyes. Then, the mice were placed 1 to 2 mm in front of the confocal scanning laser ophthalmoscope (cSLO) device, which had a built-in light source for stimulating projections. A platinum ring electrode was placed on the cornea. The multifocal electroretinogram (mf-ERG) was recorded using the RETI scan electrophysiological system (RETI scan; Roland Consult, Wiesbaden, Germany). The waveform of mf-ERG is a biphasic wave with a negative initial value followed by a positive peak, and a secondary negative phase wave, which were named as N-1, P-1, and N-2 waves, respectively. An mf-ERG can stimulate 19 regions of the retina at the same time, obtain the electrical response of each region of the retina in a short time, and extract the electrical response of each part of the retina to form a 3D ERG map.

Optical Coherence Tomography and Fundus Photography

Mice were anaesthetized by intraperitoneal injection of 5% chloral hydrate (0.0008 mL/g). The compound tropicamide eye drops were added to dilate the eyes. The mice were fixed on the test table of a Phoenix Micron IV Retinal Imaging system (Microscope; Phoenix Micron, Bend, OR, USA). The researcher adjusted the detecting lens and then started scanning. Mouse pupils were aligned with optical coherence tomography (OCT) probes and light angles were adjusted to obtain clear retinal images. The fundus photograph was simultaneously captured at the precise location in the 30 degrees circle around the optic nerve head. After scanning, the mice were transferred on the heating blanket until they woke up.

Hematoxylin and Eosin Staining

Mouse eyeballs were fixed in paraformaldehyde at 4°C for 24 hours. The cornea, lens, and iris tissues were removed under a stereo-microscope (SZ61; Olympus, Manila, Philippines). The retained eyecup was dehydrated in a fully automated dehydrator (VIP-5-J R-JC2; SAKURA, Tokyo, Japan) after being embedded in paraffin (TEC 5 EM JC-2; SAKURA). Then, the retinal specimen was cut into sections with 4 µm thickness (RX-860; YAMATO, Tokyo, Japan). Paraffin sections were dehydrated, and stained by hematoxylin and eosin (H&E). A microscope (BX53; Olympus, Tokyo, Japan) was used for observing the retinal histology. At a distance of 200 to 300 µm from the optic nerve, a clear visual field photograph was taken with a 40 × objective lens. ONL thickness in each image was quantified using ImageJ software (National Institutes of Health [NIH], Bethesda, MD, USA).

Reactive Oxygen Species Detection

The eyecup was dehydrated for 30% sucrose and embedded in the optimal cutting temperature compound (tissue-Tek; Sakura, Torrance, CA, USA). The retinal specimen was cut vertically into sections using a Leica CM1900 cryostat (Leica, Wetzlar, Germany). The ROS production was evaluated by dihydroethylamine (DHE; BBoxiProbe, BB-470516) staining. The DHE fluorescence probes were diluted 2000 times with pure water to prepare for the dye probe working solution. Each section was incubated with DHE at 37°C for 30 minutes, and then rinsed with PBS for 5 minutes × 3 times. Retinal sections were photographed at 40x magnification using a fluorescence microscope and quantified using ImageJ software.

The TUNEL assay

The TUNEL assay was performed according to the manufacturer's protocol (11684817910; Roche, Mannheim, Germany). Frozen sections were washed with PBS 3 times and then incubated with the TUNEL reaction mixture for 1 hour at 37°C. Then, the retinal sections were incubated with 10 µl DAPI for 3 minutes at room temperature, washed with PBS for 5 minutes × 3 times, sealed with anti-fluorescence quenching solution (ab104135; Abcam), and photographed under fluorescence microscope.

Immunofluorescence

Frozen retinal sections were used for immunostaining. At room temperature, the optical cutting temperature embedding agent was cleaned with PBS for 5 minutes × 3 times, and the immunohistochemical pen was used to draw circles around the tissues. The cell membrane was penetrated with a penetrating agent (1% Triton X-100 in PBS) and closed with 3% bovine serum (3% BSA in PBS containing 0.1% Triton X-100) at 37°C for 30 minutes. Then, the retinal sections were incubated with primary antibody indulging IBA1 (ab178847, 1:100; Abcam), GFAP (G3893, 1:200; Sigma), Rhodopsin (ab98887, 1:500; Abcam), CX3CL1 (ab25088, 1:500; Abcam), CX3CR1 (2093, 1:500; ProSci), GS (ab176562, 1:250; Abcam), Ly6G (ab25377, 1:100; Abcam,) at 4°C overnight. The retinal section was cleaned with PBS for 5 minutes × 3 times, and then were incubated with second antibody anti-Mouse Alexa 488 (ab6785, 1:1000; Abcam), anti-Ribbit Alexa 488 (ab150077, 1:1000; Abcam), or anti-Rat Alexa 488 (ab150157, 1:200; Abcam) for 1 hour at 37°C. Retinal sections were washed with PBS for 5 minutes × 3 times, and incubated with anti-fluorescence quenching containing DAPI (D21490; Thermo Fisher Scientific). A computer-assisted imaging analysis system (ImageJ; NIH, USA) was used to quantify the intensity of immunofluorescence. Relative protein expression levels were normalized to the control group by calculating fluorescence intensity.

Western Blot Assay

Extracted retina protein was measured using the BCA Protein Concentration Assay Kit (P0010; Beyotime, China). Protein samples were adjusted to the same protein concentration (1 µg/µL) and denatured. Each sample (10 µL) containing an equal amount of protein was extracted for electrophoresis. Proteins were transferred to polyvinylidene difluoride (PVDF) membranes (Millipore, Billerica, MA, USA)

Investigative Ophthalmology & Visual Science

in transfer buffer. PVDF membranes were blocked with 5% skimmed dry milk (5% bovine serum) for 2 hours at room temperature, and then were washed with PBS containing 0.1% Tween-20 (TBST) for 5 minutes × 3 times, with separate primary antibodies IL-1β (12224, 1:1000; Cell Signaling Technology), TNF-α (ab6671, 1:1000; Abcam), NF-κB (8242, 1:1000; Cell Signaling Technology), p-NF-κB (3033, 1:1000; Cell Signaling Technology), CX3CL1 (ab25088, 1:1000; Abcam), CX3CR1 (ab66712093, 1:1000; ProSci) GAPDH (ab8245, 1:20,000; Abcam), β-actin (A1978, 1:10,000; Sigma) overnight at 4°C. The primary antibody was recovered, and the PVDF membrane was washed with TBST for 5 minutes × 4 times, and then was incubated with goat anti-Mouse IgG secondary antibody (ab6789, 1:10,000; Abcam) or goat anti-Rabbit IgG secondary antibody (ab6721, 1:20,000; Abcam) for 2 hours at room temperature. After four washes with TBST, the electrochemiluminescence (ECL) droplets were added to the PVDF membrane to uniformly distribute over the whole surface of the membrane, and then put into the gel imaging system for photography.

Statistical Analysis

Statistical analysis was performed using GraphPad Prism 7.0 edition. The statistical data were tested for normality by 1-way ANOVA analysis and Bonferroni multiple comparison. The data were expressed as mean ± standard deviation (mean ± SD). $P < 0.05$ was statistically significant.

Results

Photoreceptor Apoptosis in the Retina of the RD Model

In the normal controls, the ONL was complete, and the boundary between retinal layers was even. Inter segments/outer segments (IS/OS) of the photoreceptor were neatly arranged and their nucleus were uniformly stained with H&E (Fig. 1A). Conversely, in the RD model, the retinal thickness and the cell number in ONL decreased progressively between P7 and P28 after modeling (Fig. 1B; $P < 0.0001$, $n = 6$). The ONL structure was bent and the boundary between IS/OS was blurred. Brown deposits were detected in the RPE of the RD model (marked with the white arrow), and the lesion scale increased over time. These brown deposits were similar to the drusen lipids in patients with RD in terms of appearance. As shown in the immunostaining of rhodopsin, a specific rod photoreceptor marker, the architecture of IS/OS, were neat at P1. Subsequently at P7, the rod photoreceptors were severely damaged and theirs IS/OS were shortened. The fluorescence intensity of rhodopsin decreased over time (Fig. 1C; $P < 0.0001$, $n = 6$). Moreover, the intensity of ROS staining increased significantly after modeling (Fig. 2A; $P < 0.0001$, $n = 6$), indicating that excessive oxidation occurred in the retina of RD model. Furthermore, the TUNEL positive cells appeared in the ONL of the RD model at P7, and the cell counts increased over time (Fig. 2B; $P < 0.0001$, $n = 6$).

CX3CL1/CX3CR1 Activation in the Retinas of the RD Model

Microglia cells in the retinal sections of the RD model were labeled by ionized calcium binding adapter molecule 1 (IBA1). At P1, the microglia cells were distributed in IPL and OPL with a ramified shape. Subsequently at P7, the microglia cells migrated to the ONL and assumed an "amoeba" shape. Quantification analysis showed that the counts of IBA1 positive cells peaked at P14 (Fig. 3A; $P < 0.0001$, $n = 6$). Glial fibrillary acid protein (GFAP) is a typical marker of retinal gliosis, and its expression increases with its post-translational modification of citrullination.[37] At P1, the GFAP immunostaining was distributed throughout the retina, forming the internal limiting membranes (ILMs) and external limiting membranes (ELMs). However, these Müller cells were activated to produce glial filaments at P7, and the distribution range of GFAP gradually extended to ONL. The number of GFAP-positive cells increased over time, and peaked at P14 (Fig. 3B; $P < 0.0001$, $n = 6$). Glutamine synthetase (GS) can protect the retina from glutamate excitatory toxicity by transporting extracellular glutamate, and acts as a differentiation marker of Müller cell.[38] In the RD model, GS immunostaining decayed progressively after modeling, and the distribution was disordered (Fig. 3C; $P < 0.0001$, $n = 6$). Western blot results showed that the expression levels of IL-1β and TNF-α increased significantly after modeling (Fig. 3D; $P < 0.0001$, $n = 6$). The number of CX3CL1/CX3CR1 positive cells also increased significantly at the onset of RD (Figs. 4A, 4B; $P < 0.0001$, $n = 6$). Consistent with the immunofluorescence results, the Western blot results showed that the protein levels of CX3CL1/CX3CR1 increased significantly during the RD process (Figs. 4C, 4D; $P < 0.0001$, $n = 6$). The expressions of p-NF-κB, a downstream mediator of CX3CL1/CX3CR1 pathway, also increased significantly in the RD model (Fig. 4E; $P < 0.0001$, $n = 6$).

CX3CR1 Antagonist Protected the Morphology of the RD Model

AZD8797, a CX3CR1 antagonist, was delivered into the vitreous body of the RD model. OCT examination showed that the retinal structure of the RD model was disrupted and the reflectivity increased significantly compared with normal controls. Conversely, the retina of the RD + AZD8797 group had intact structures and clear boundary between layers. The retinal thickness in the RD + AZD8797 group was significantly larger compared with the RD group (Fig. 5A; Supplementary Fig. 1A; $P < 0.0001$, $n = 6$). Fundus photography showed that the retinal vessels of normal control were distributed evenly with distinct branches and reddish color. However, pervasive and disordered lesions were found in the fundus of the RD group. After AZD8797 treatment, the scale of retinal lesions reduced significantly, and the vessel distribution was much clearer. H&E staining showed that the retinal structure of the RD + AZD8797 group was consolidated. The IS/OS length of the RD + AZD8797 group increased significantly compared with the RD group (Fig. 5B; Supplementary Fig. 1B; $P < 0.01$, $n = 6$). Immunostaining of rhodopsin showed that the rod photoreceptor in the RD + AZD8797 group had longer IS/OS compared with that of the RD group (Fig. 5C; Supplementary Fig. 1C; $P < 0.01$, $n = 6$).

CX3CR1 Antagonist Improved the Visual Function of the RD Model

In the mf-ERG examination, the mean amplitude of the P-1 waves in the normal control group were significantly larger compared with that in the RD group. The 3D ERG map also showed that severe visual malfunction occurred in the RD group. However, AZD8797 could improve the

Investigative Ophthalmology & Visual Science

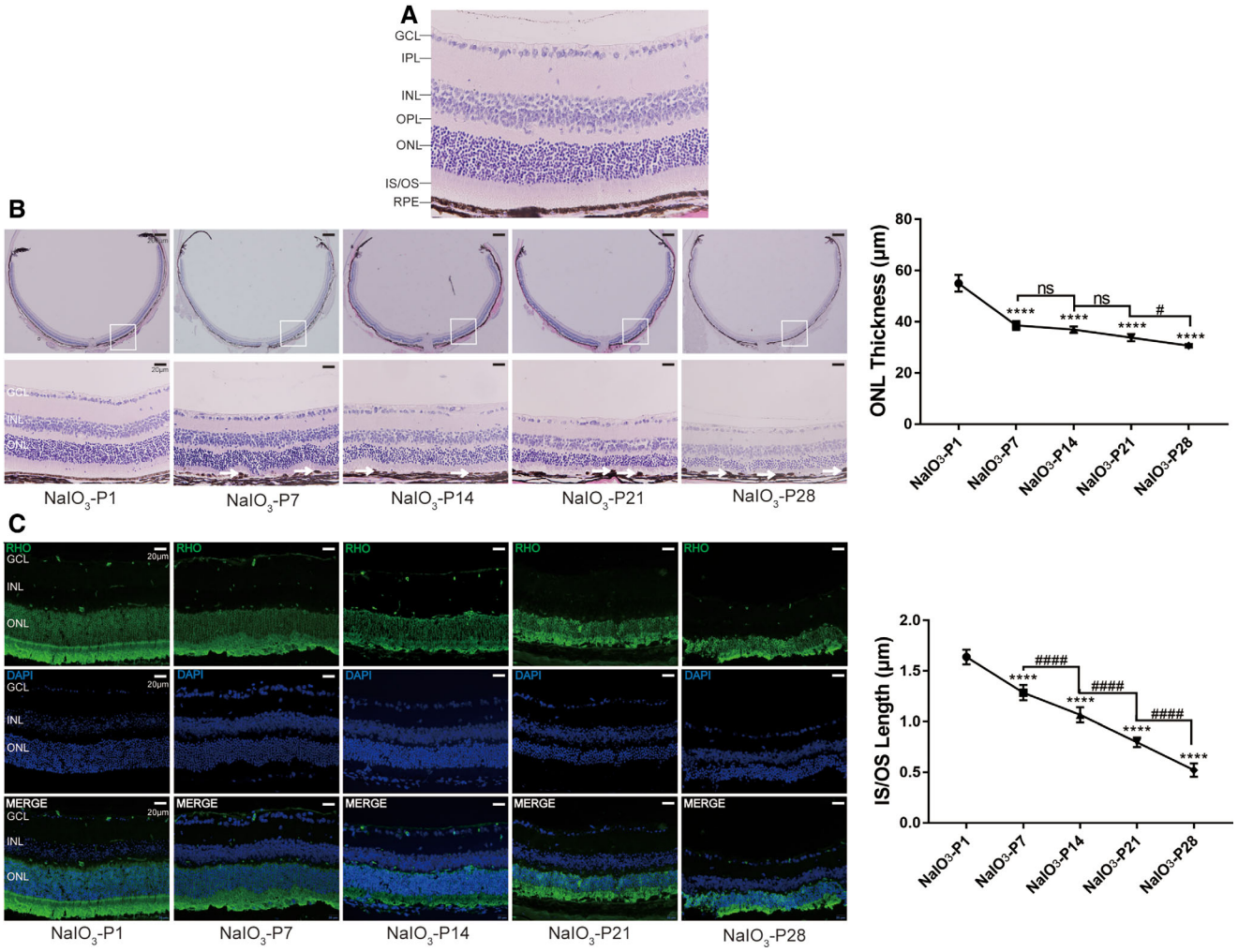

Figure 1. Photoreceptor apoptosis in the retina of the RD model. (**A**) H&E staining was performed on the retinal sections. (**B**) In the RD model, the retinal thickness and the ONL thickness decreased progressively after modeling. The ONL structure was bent and the boundary between IS/OS was blurred. Brown deposits were marked with the *white arrow*. (**C**) As shown in the immunostaining of rhodopsin, the rod photoreceptors were severely damaged and their IS/OS were shortened after modeling. The fluorescence intensity of rhodopsin decreased over time. GCL, ganglion cell layer; IPL, inner plexiform layer; INL, inner nuclear layer; OPL, outer plexiform layer; ONL, outer nuclear layer; IS/OS, inner segment rod/outer segment rod; RPE, retinal pigment epithelium. (Scale = 400 μm and 20 μm, $^{*}P < 0.05$, $^{**}P < 0.01$, and $^{****}P < 0.0001$, for differences between time points, $^{\#}P < 0.05$, $^{\#\#}P < 0.01$, $^{\#\#\#}P < 0.001$, and $^{\#\#\#\#}P < 0.0001$ for differences between animal groups, $n = 6$).

retinal function comprehensively (Figs. 6A, 6B; Supplementary Figs. 2A, 2B; $n = 6$). In the RD + AZD8797 group, the amplitude of P-1 waves increased significantly in the all the 3 rings compared with the RD group. Subentry, the mice in the RD + AZD8797 group were subjected to light/dark box test. The behavioral parameters including movement speed and shuttle times between boxes in the RD + AZD8797 group increased significantly compared with those in the RD group. On the other hand, the movement time and distance in the light box reduced significantly after AZD8797 treatment (Figs. 7A, 7B; Supplementary Fig. 3A; $P < 0.01$, $n = 8$). In the open field test, behavioral parameters including the frequency of entering the central area, the duration in the central area, the total distance, and speed of movement in the RD + AZD8797 group increased significantly compared with those in the RD group (Figs. 7C, 7D; Supplementary Fig. 3B; $P < 0.01$, $n = 8$). In greater detail, the spatial vision of mice was quantified according to their optomotor response.[39] The results showed that the contrast sensitivity and spatial resolution of the RD group was significantly lower compared with normal controls. However, the RD + AZD8797 group mice had better visuomotor response in terms of contrast sensitivity and spatial resolution (Fig. 8; Supplementary Fig. 4A; $P < 0.0001$, $n = 6$). These findings indicated that AZD8797 could improve the visual function and behavioral performance of the RD model.

CX3CR1 Antagonist Alleviated Oxidative Stress and Apoptosis in the RD Model

DHE fluorescence assay showed that the ROS level in the RD group increased significantly compared with the normal control group (Fig. 9A; $P < 0.0001$, $n = 6$). However, AZD8797 could mitigate the ROS production in degenerative retinas (see Fig. 9A; Supplementary Fig. 5A; $P < 0.001$, $n = 6$). Moreover, the TUNEL assay showed that the number of

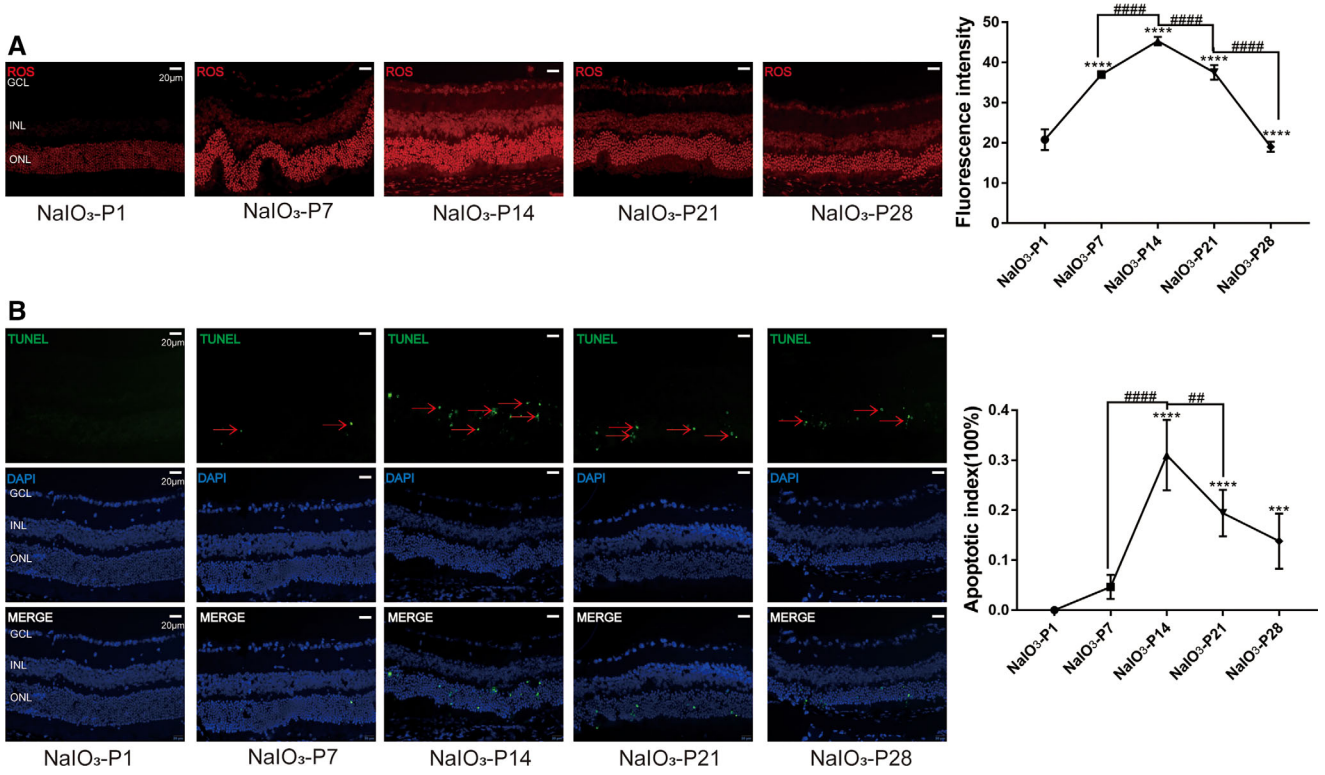

Figure 2. Oxidative stress and photoreceptor apoptosis in the retina of RD model. (**A**) The intensity of ROS staining increased significantly after modeling. (**B**) The TUNEL positive cells were detected in the ONL of RD model at P7, and the cell counts increased progressively. (Scale = 20 μm), the *red arrows* indicate TUNEL positive cells. ($^{*}P < 0.05$, $^{**}P < 0.01$, and $^{****}P < 0.0001$, for differences between time points, and $^{\#}P < 0.05$, $^{\#\#}P < 0.01$, $^{\#\#\#}P < 0.001$, and $^{\#\#\#\#}P < 0.0001$, for differences between animal groups, $n = 6$).

apoptotic cells in the RD + AZD8797 group reduced significantly compared with the RD group (Fig. 9B; Supplementary Fig. 5B; $P < 0.001$, $n = 6$). These results suggested that AZD8797 enhanced the photoreceptor survival in the RD model through alleviating the oxidative stress and apoptosis.

CX3CR1 Antagonist Inhibited the Neuralgia Activation and Inflammatory Response

As shown in the immunochemistry assay, the microglia cells in the retina of the RD group were activated with the amoeboid-like shape. However, microglia cell activation was inhibited by AZD8797 treatment, as evidenced by the reduced the number of IBA1 positive cells (Fig. 10A; Supplementary Fig. 6A; $P < 0.01$, $n = 6$). Then, we used Ly6G to label the neutrophils in the retina. The results showed that the number of Ly6G positive cells in the retina of the RD model increased significantly compared with that in the normal controls. However, AZD8797 treatment reduced significantly the number of Ly6G positive cells in the retina of RD model (Fig. 10B; $P < 0.0001$, $n = 6$). Moreover, the microglia cells in the RD + AZD8797 group were distributed within the inner retinal layers with branching structure. In the RD group, the immunostaining of GFAP increased significantly compared with the normal controls. After AZD8797 treatment, the immunostaining intensity of GFAP reduced significantly (Fig. 10C; Supplementary Fig. 6B; $P < 0.0001$, $n = 6$). On the other hand, the GS immunostaining in the RD + AZD8797 group increased significantly compared with the RD group (Fig. 10D; Supplementary Fig. 6C; $P < 0.01$, $n = 6$). Western blot results showed that the IL-1β and TNF-α protein expressions reduced significantly after AZD8797 treatment (Fig. 10E; Supplementary Fig. 6D; $P < 0.001$, $n = 6$).

In the retinas of the RD + AZD8797 group, the number of CX3CL1 and CX3CR1 positive cells reduced significantly compared with the RD group (Figs. 11A, 11B; Supplementary Fig. 7A, 7B; $P < 0.001$, $n = 6$). Western blot results showed that the protein levels of CX3CL1 and CX3CR1 in the RD + AZD8797 group reduced significantly compared with the RD group (Figs. 11C, 11D; Supplementary Fig. 7C, 7D; $P < 0.0001$, $n = 6$). Additionally, the expression level of p-NF-κB protein decreased significantly after AZD8797 treatment (Fig. 11E; Supplementary Fig. 7E; $P < 0.01$, $n = 6$).

Discussion

In RD pathogenesis, excessive oxidative stress, disrupted protein balance, and mitochondrial dysfunction form an internal feedback loop that allows the accumulation of abnormally misfolded proteins and lipids.[40] Drusen is composed of oxidized lipids, lipofuscin, complement, and other immune-activating components. Accumulating evidence shows that these constituents will induce chronic inflammation in the subretinal space.[41,42] Accordingly, the degree of photoreceptor demise exacerbates with the enlargement of drusen size.[43] In this study, we show that the pathological features of the RD model, including focal retina atrophy, lipofuscin accumulation, and progressive visual impairments, all closely resemble these occurring in patients.[44] In particular, the microglia and Müller cell are activated to release inflammatory factors into the retina

Investigative Ophthalmology & Visual Science

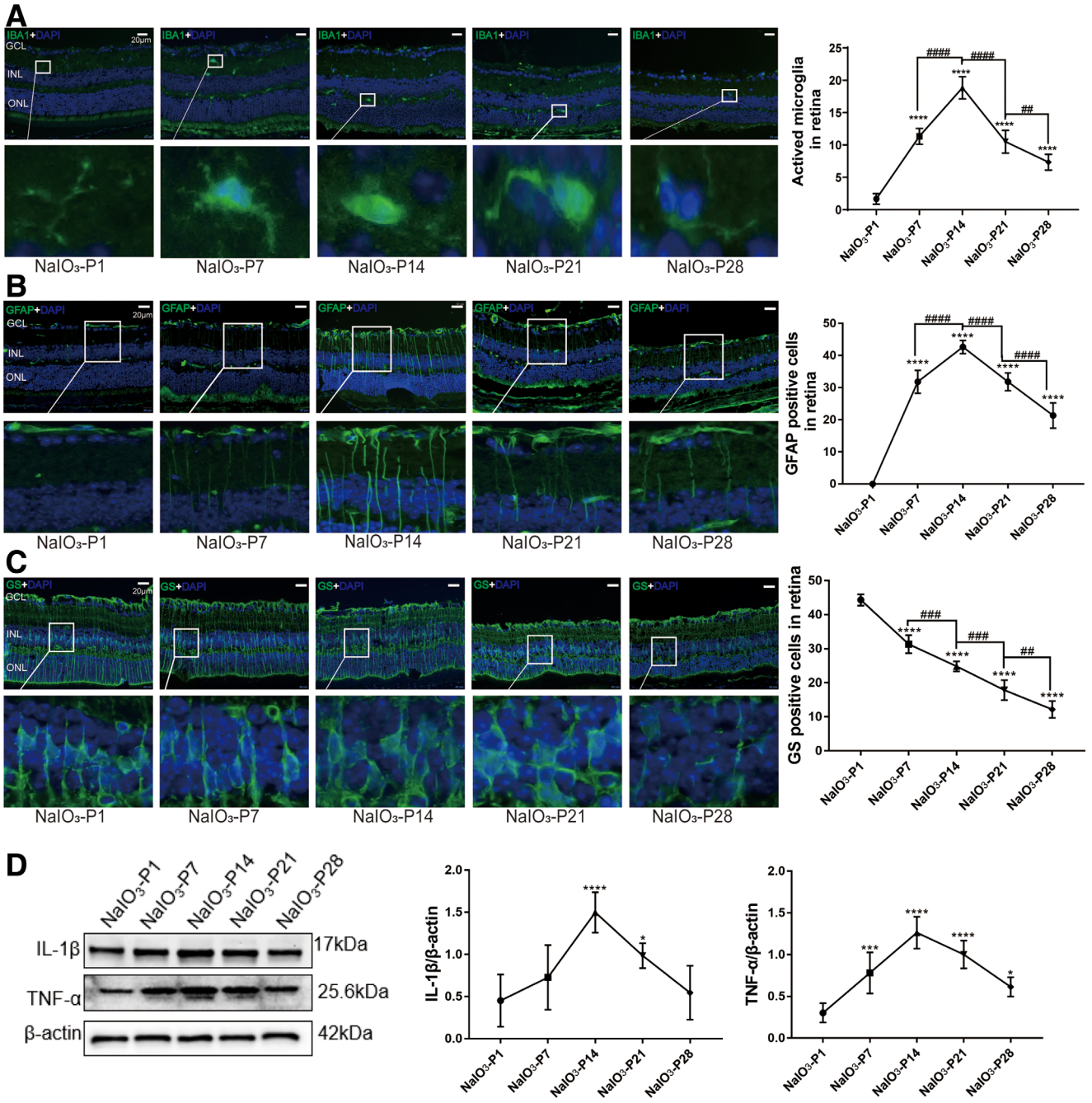

Figure 3. Neuroglia activation in the RD model. (**A**) Microglia in the retinas of RD model were labeled with IBA1. The microglia were distributed in IPL and OPL with a ramified shape. At P7, the microglia migrated to the ONL and assumed an "amoeba" shape. Quantification analysis showed that the counts of IBA1 positive cells peaked at P14. (**B**) The GFAP immunostaining showed that Müller cells were activated to produce glial filaments at P7, and the distribution range of GFAP gradually extended to ONL. The number of GFAP-positive cells increased over time. (**C**) GS immunostaining decayed progressively after modeling, and the distribution was disordered. (**D**) Western blot results showed that the IL-1β and TNF-α expressions increased significantly after modeling. ($^{*}P < 0.05$, $^{**}P < 0.01$, and $^{****}P < 0.0001$, for differences between time points, and $^{\#}P < 0.05$, $^{\#\#}P < 0.01$, $^{\#\#\#}P < 0.001$, and $^{\#\#\#\#}P < 0.0001$, for differences between animal groups, $n = 6$).

tissue of the RD model. The CX3CL1/CX3CR1 signaling pathway, which plays a critical role in modulating microglia activity, is upregulated throughout the whole degenerative process of the RD model.

It is widely acknowledged that microglia-mediated inflammation contributes to the pathogenesis of RD.[45] In both human patients and RD animal models, chronic pro-inflammatory responses engineered by microglia cells are considered as an initiative event in retinal damage.[46] After activation, these amoeba-like microglia cells release neurotoxic molecules, such as pro-inflammatory cytokines, ROS intermediates, and proteinases to exacerbate photoreceptor death.[47] Microglia cells represent a population of macrophages that engage in the activities of immune surveillance and maintaining endogenous homeostasis.[48] They can phagocytose the shedding membrane discs and the cellular debris from dying photoreceptors.[49] When the retina is exposed to exogenous insults, microglia cells can respond

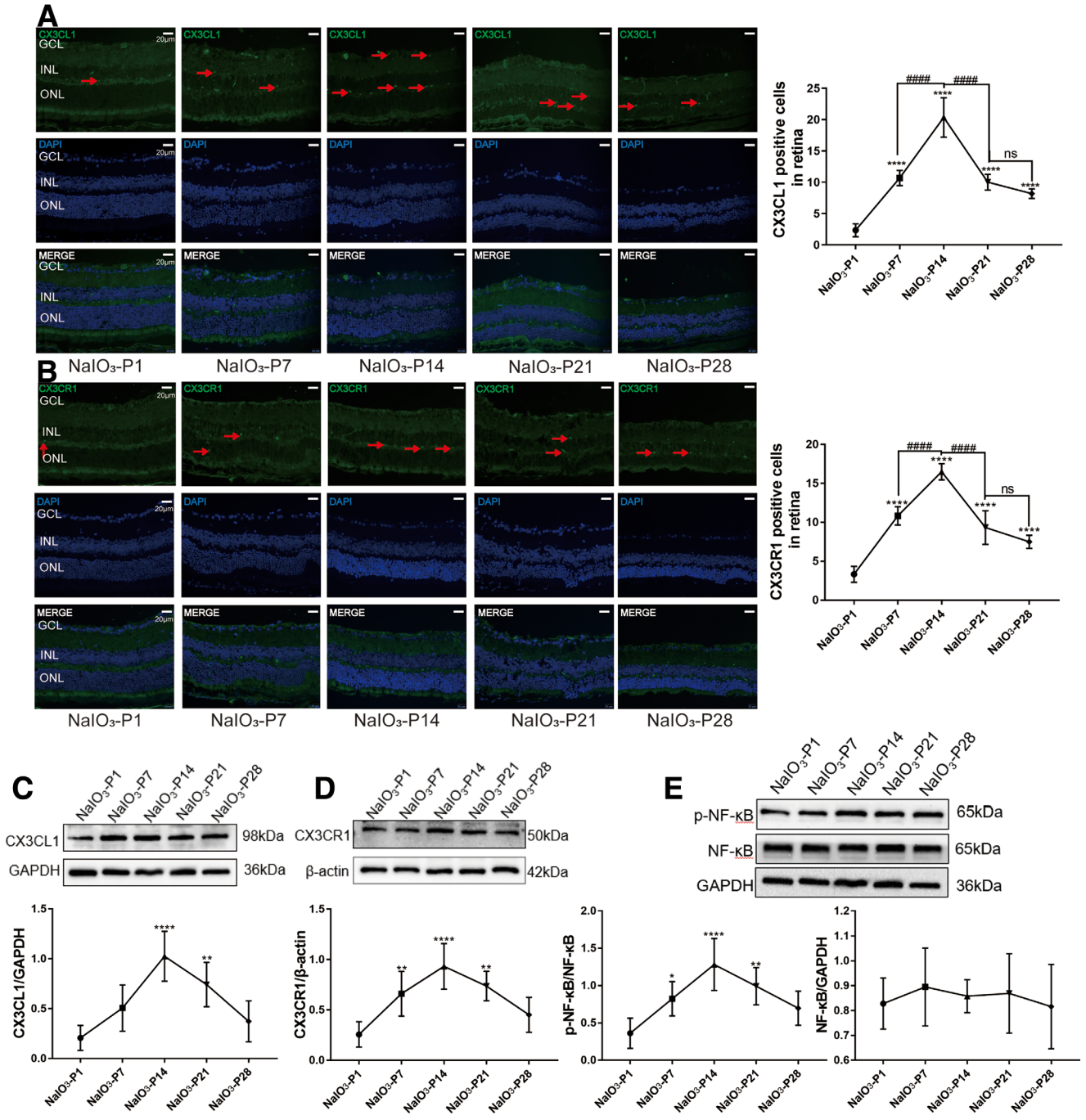

Figure 4. CX3CL1-CX3CR1 signaling activation in the retina of RD model. (**A** and **B**) The number of CX3CL1/CX3CR1 positive cells increased significantly at the onset of RD. (**C** and **D**) The protein levels of CX3CL1/CX3CR1 increased significantly during the RD process. The expressions of p-NF-κB, a downstream mediator of CX3CL1/CX3CR1 pathway, also increased significantly in the RD model. (**E**) ($^{*}P < 0.05$, $^{**}P < 0.01$, and $^{****}P < 0.0001$, for differences between time points, and $^{\#}P < 0.05$, $^{\#\#}P < 0.01$, $^{\#\#\#}P < 0.001$, and $^{\#\#\#\#}P < 0.0001$, for differences between animal groups, $n = 6$).

dynamically to pathological factors. In this study, we show that these amoeboid-like microglia cells migrate into the ONL of the RD model. The accumulation of congenital immune cells in the ONL or subretinal space has been recognized as a typical hallmark of RD progression.[50] Prolonged exposure to activation stress will cause microglia to denature retinal neurons.[51] Encouragingly, the intravitreal injection AZD8797 can inhibit the microglia activation and migration in the RD model. AZD8797 also mitigates the expression levels of IL-1β and TNF-α in the retina tissue. Thus far, several broad-spectrum antibiotics have been shown to prevent complement activation, inhibit matrix metalloproteinases, and inhibit microglia activation in the RD model.[52,53] For instance, minocycline can reduce significantly microglial activation and migration in Royal College of Surgeons (RCS) mice.[54] Once the microglia activation has been suppressed by anti-inflammatory treatment, the retinal structure and visual function are efficiently preserved.

Investigative Ophthalmology & Visual Science

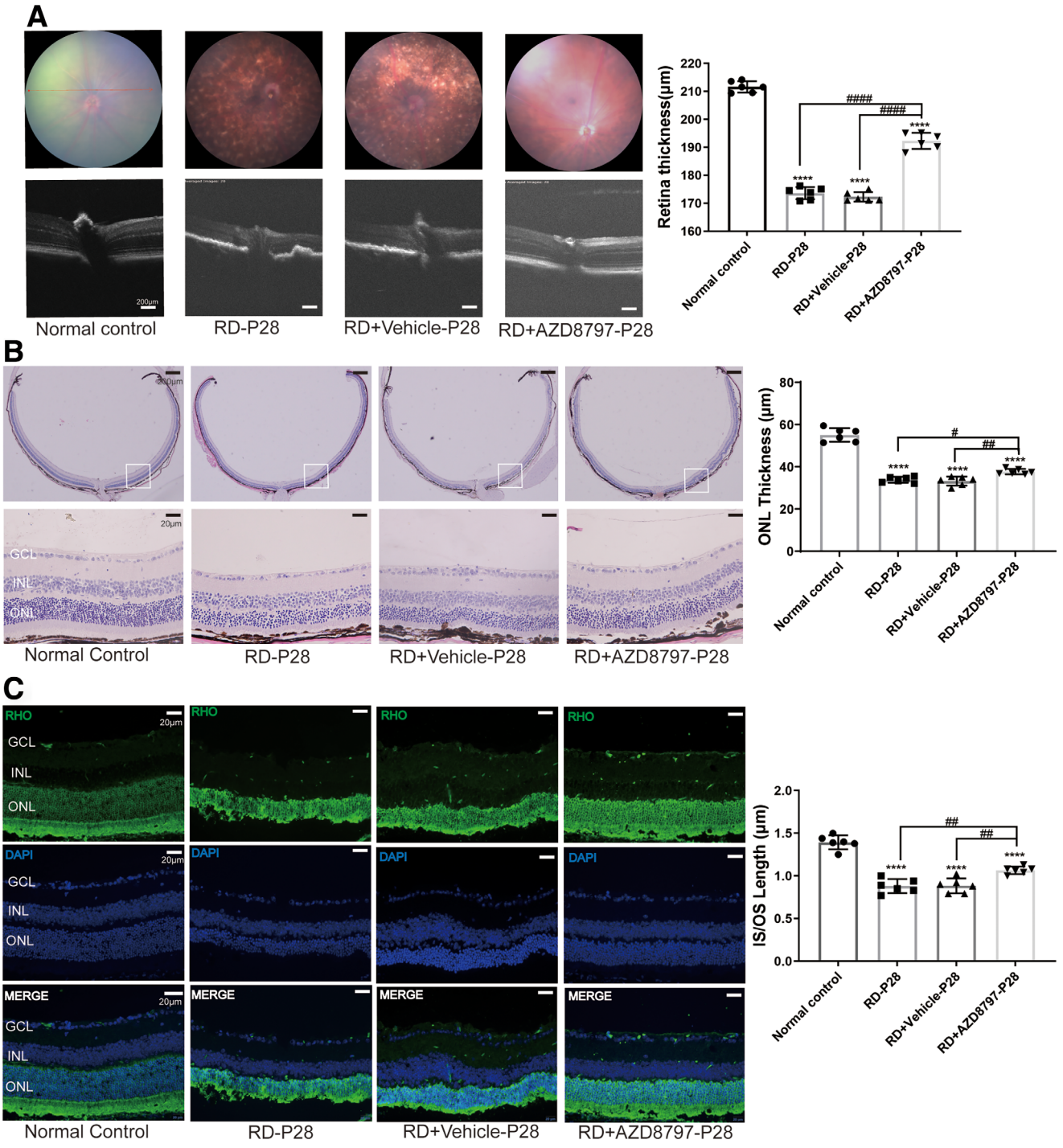

Figure 5. AZD8797 alleviates the morphology retinal in RD mice model at P28. (**A**) OCT examination showed that the retina of the RD + AZD8797 group had intact structures and clear boundary between layers. The retinal thickness in the RD + AZD8797 group was significantly larger compared with the RD group. Fundus photography showed that the scale of retinal lesions reduced significantly after AZD8797 treatment. (**B**) H&E staining showed that the ONL thickness of the RD + AZD8797 group increased significantly compared with the RD group. (**C**) Immunostaining of rhodopsin showed that the rod photoreceptor in the RD + AZD8797 group had longer IS/OS compared with that of the RD group. (*$P < 0.05$, **$P < 0.01$, and ****$P < 0.0001$, for differences compared with the normal control, and $^{\#}P < 0.05$, $^{\#\#}P < 0.01$, $^{\#\#\#}P < 0.001$, and $^{\#\#\#\#}P < 0.0001$, for differences between animal groups, $n = 6$).

Moreover, intravitreal injection of anakinra, a recombinant IL-1 receptor antagonist (IL-1RA), can alleviate photoreceptor apoptosis in *rd10* mice.[55] Furthermore, translocator protein (TSPO) is a diazepam-binding inhibitor that can bind with its endogenous ligand in the eye. It can eliminate the activated M1 microglia and inhibiting the release of TNF, thereby significantly attenuating the photoreceptor loss.[56] Taken together, these findings highlighting that medications targeting microglia activation might be effective to arrest the photoreceptor demise in RD. CXCR2 is a

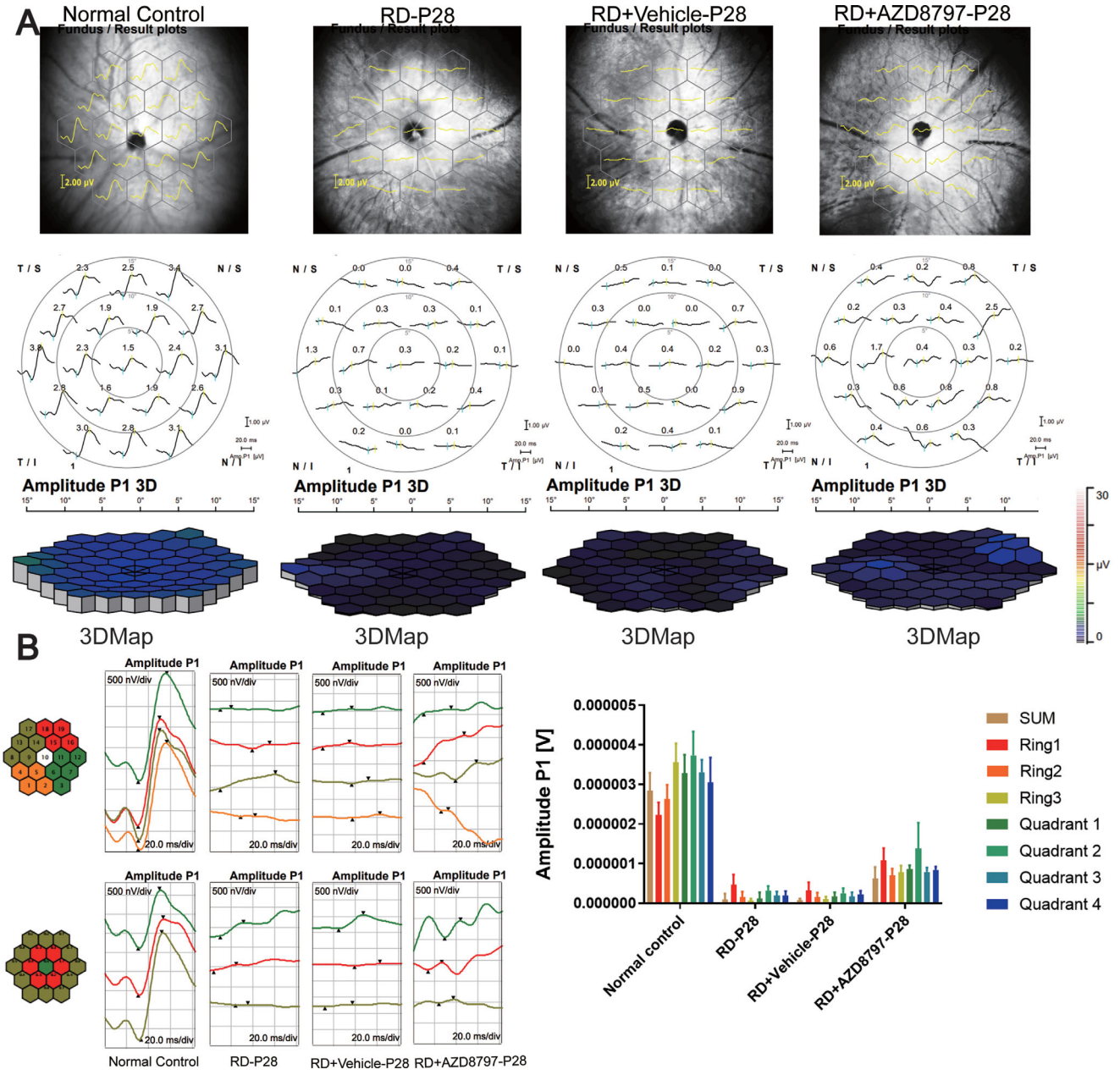

Figure 6. AZD8797 improved the ERG function in RD model at P28. (**A**) The typical ERG waveforms and 3D ERG map of each animal groups at P28. (**B**) Representative images of amplitude changes in all the four quadrants: superior temporal, inferior, and nasal quadrants, respectively, statistical analysis of the amplitudes in three recording rings: central, mid-pericentral, and peripheral rings, respectively. In the RD + AZD8797 group, the amplitude of P-1 wave increased significantly in the all the quadrants and rings compared with the RD group.

G-protein coupled receptor (GPCR) responsible for the cellular signal transduction.[57] CXCR2 can be activated by interleukin-8 (IL-8), thereby regulating the recruitment of neutrophils from blood to the inflammatory sites.[58] Increased neutrophil infiltration has been found in the retinas of patients with dry/atrophic age-related macular degeneration (AMD) and mice models.[59,60] On the other hand, the blockade of CXCR2 markedly can attenuate the macrophage infiltration, proinflammatory cytokine release, and oxidative stress in the hypertensive retinopathy mouse model.[61] In our study, we show that AZD8797 can inhibit CXCR2 mediated neutrophil chemotaxis, and ameliorate the inflammation reaction in degenerative retinas. These findings suggest that therapeutic agents seeking to inhibit the neutrophil chemotaxis may be effective to ameliorate the neural and vascular damages in RD.

Müller cells constitute the extracellular ATP source and mediate the dynamic process of retinal gliosis.[62] Typical features of retinal gliosis include the Müller cells hypertrophy, enhanced intermediate filament production (such as GFAP), increased rates of proliferation, and reduced GS expression.[3] Mark et al. have shown that retinal laser injury stimulates Müller cell activation as indicated by upregulation of the GFAP and nesting.[63] Enhanced GFAP has also been found in the RP model, a retinitis pigmentosa model.[64] The upregulation of GFAP can help to

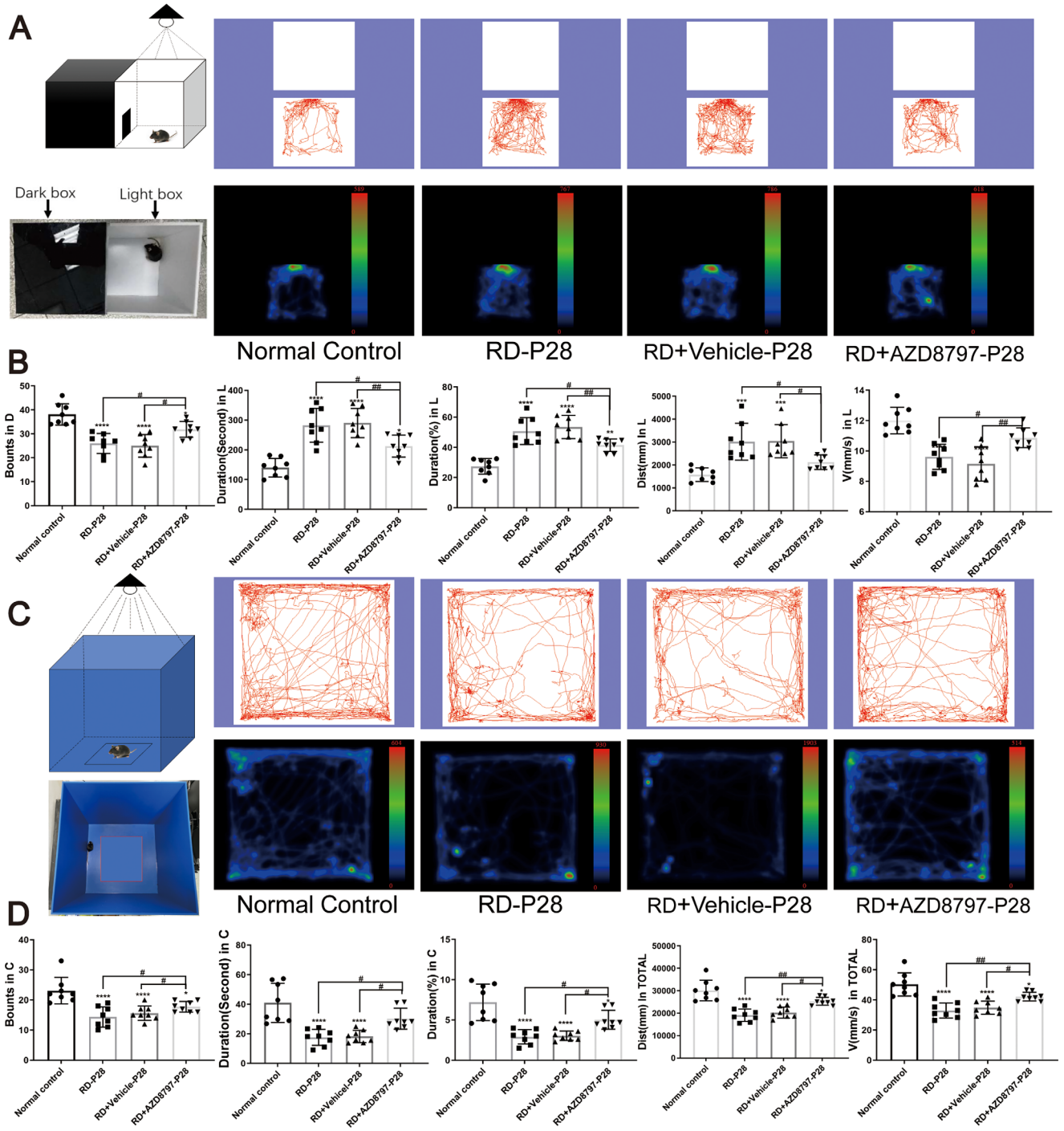

Figure 7. AZD8797 alleviated the behavioral impairments of RD model at P28. (**A** and **B**) Light/dark box test (trajectories and density maps) of the mice after AZD8797 treatment at P28. The statistical results of behavioral parameters including the shuttle through in the dark box, durations in the light box, the distance traveled in the light box, and the speed of movement of mice in the light box. (**C** and **D**) Open field test of (trajectories and density maps) of the mice after AZD8797 treatment at P28. The statistical results of behavioral parameters including shuttle through in the center area, durations(s) in the center area, durations (%) in the center area, the distance traveled in the center area, and the speed of movement of mice in the center area ($^{*}P < 0.05$, $^{**}P < 0.01$, and $^{****}P < 0.0001$, for differences compared with the normal control, and $^{\#}P < 0.05$, $^{\#\#}P < 0.01$, and $^{\#\#\#\#}P < 0.0001$, for differences between animal groups, $n = 8$).

maintain the integrity of retinal tissue by facilitating the cyto-architectural remodeling. However, prolonged GFAP expression will produce passive effects on the survival of retinal neurons.[65] For instance, over-activated Müller cells secrete TNF-α, which interacts with interleukin chemokines and promote microglia infiltration into the outer layers of retina. The intermediate filament of Müller cells also acts as an adhesive cellular scaffold that guides the movement of the reactive microglia across various retinal layers.[66] Additionally, hypertrophied side branches of Müller cells can

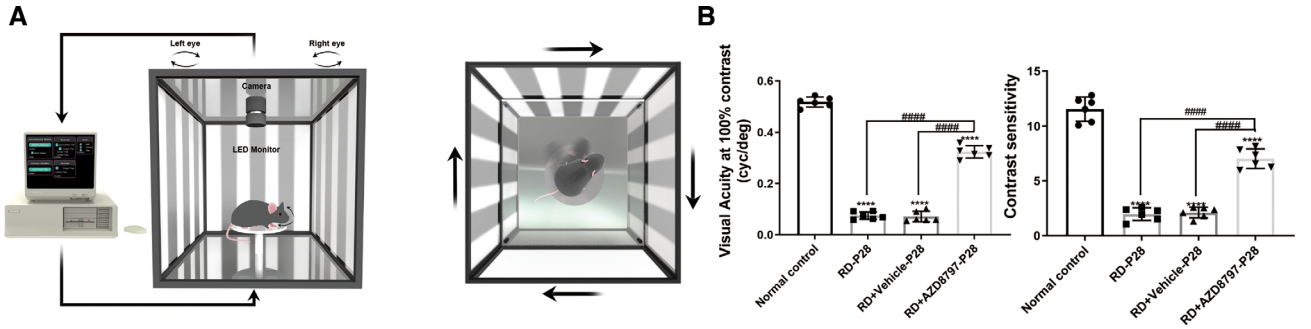

Figure 8. AZD8797 improved visuospatial behavior of RD model at P28. (**A**) Schematic diagram of visuospatial behavior test. (**B**) AZD8797 improved the spatial resolution and contrast sensitivity of the RD model at P28 ($n = 6$). (*$P < 0.05$, **$P < 0.01$, and ****$P < 0.0001$, for differences compared with the normal control, and $^{\#}P < 0.05$, $^{\#\#}P < 0.01$, $^{\#\#\#}P < 0.001$, and $^{\#\#\#\#}P < 0.0001$, for differences between animal groups, $n = 6$).

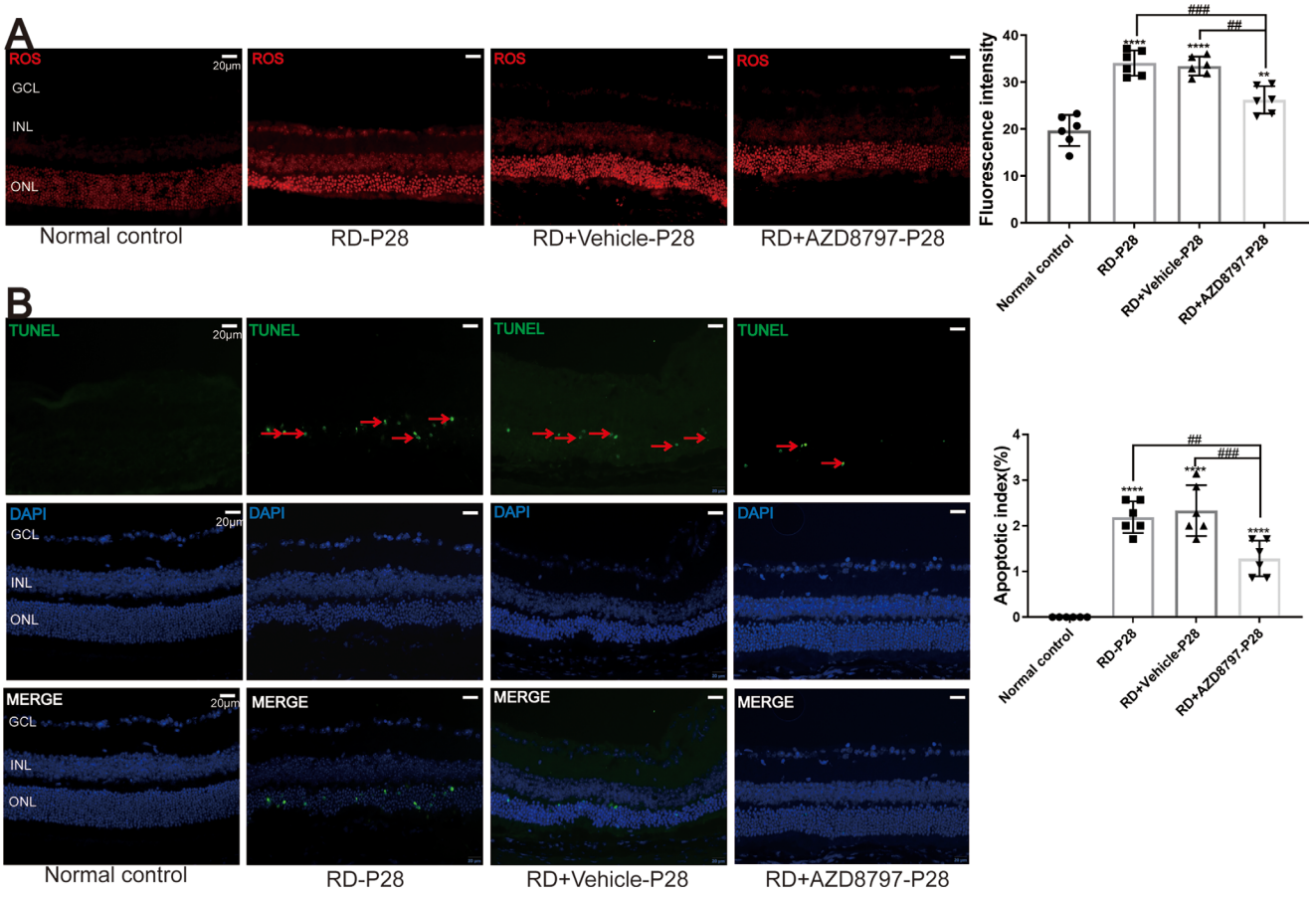

Figure 9. AZD8797 alleviated oxidative stress and photoreceptor apoptosis in RD model at P28. (**A**) DHE fluorescence assay showed that AZD8797 could mitigate the ROS production in degenerative retinas. (**B**) TUNEL assay showed that the number of apoptotic cells in the RD + AZD8797 group reduced significantly compared with the RD group, the *red arrows* indicated the TUNEL positive cells. (*$P < 0.05$, **$P < 0.01$, and ****$P < 0.0001$, for differences compared with the normal control, and $^{\#}P < 0.05$, $^{\#\#}P < 0.01$, $^{\#\#\#}P < 0.001$, and $^{\#\#\#\#}P < 0.0001$, for differences between animal groups, $n = 6$).

enter the outermost photoreceptor layer and disturb the normal metabolism.[67] Therefore, excessive gliosis reaction would be deleterious to retinal neurons. Encouragingly, AZD8797 inhibits the Müller cell mediated gliosis response, as evidenced by reduced GFAP expression and increased GS level. Previous researchers have proposed that modulating the Müller cell activity can enhances the survival of photoreceptors. For instance, silencing AQP4-AS1 can inhibit the Müller cell mediated gliosis in the DR mice model, thereby alleviating the retinal capillary degeneration and retinal ganglion cells (RGC) demise.[68] In the traumatic proliferative vitreoretinopathy (PVR) rabbit model, a slow-release dexamethasone implant can promote photoreceptor survival by mitigating Müller cell gliosis.[69] Recent studies also show that photobiomodulation (PBM) inhibits Müller cell activation and reduce the expression level of IL-1β and IL-6 in

Investigative Ophthalmology & Visual Science

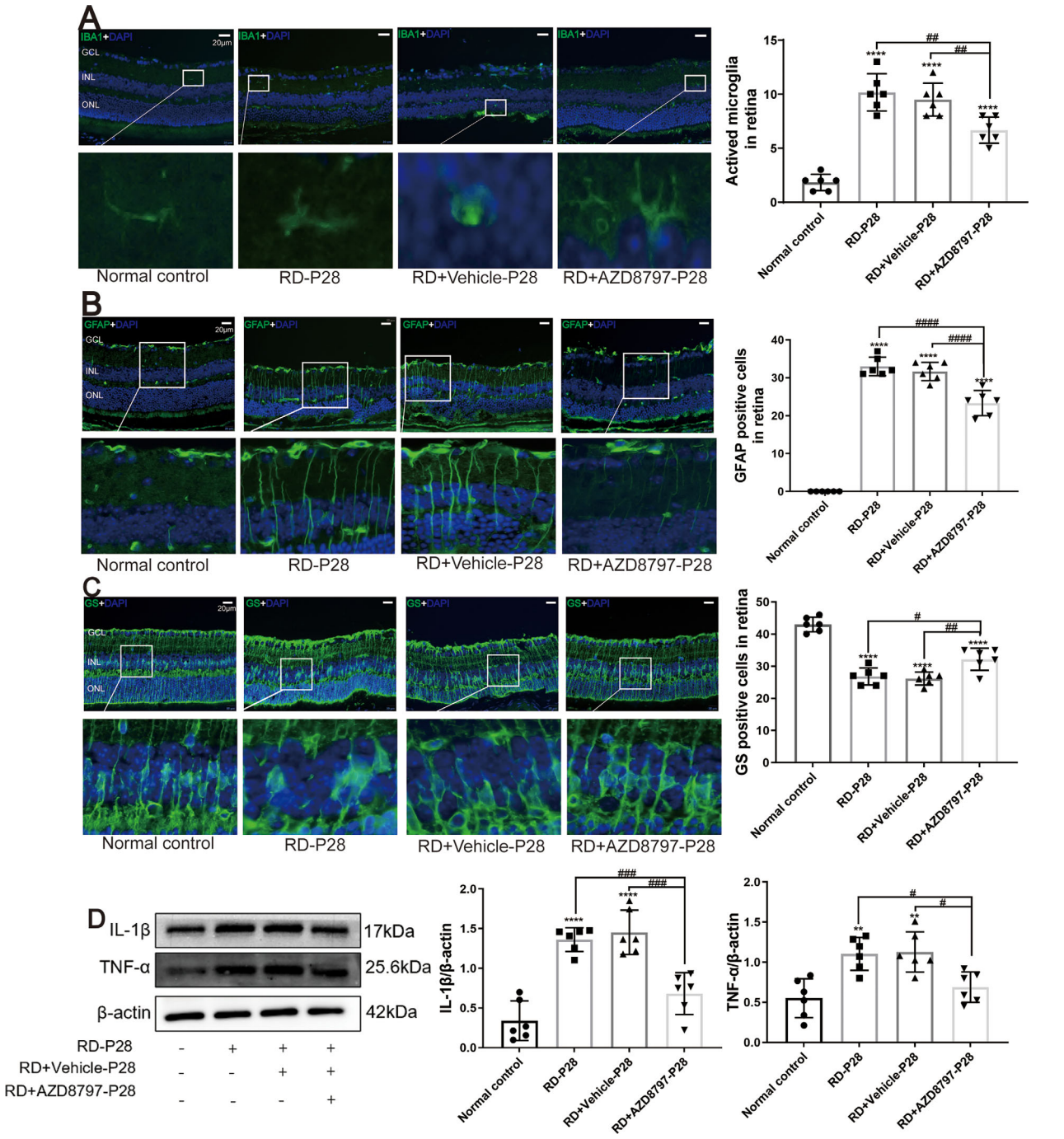

Figure 10. AZD8797 inhibited the neuroglia activation and inflammatory response. (**A**) The microglia cells in the RD + AZD8797 group were distributed within the inner retinal layers with branching structure. The number of IBA1 positive cells in the RD + AZD8797 group reduced significantly compared with the RD group. (**B**) The number of Ly6G-positive cells in the RD group reduced significantly after AZD8797 treatment. (**C**) The immunostaining intensity of GFAP in the RD group reduced significantly after AZD8797 treatment. (**D**) The GS immunostaining in the RD + AZD8797 group increased significantly compared with the RD group. (**E**) Western blot results shown that the IL-1β and TNF-α protein expressions reduced significantly after AZD8797 treatment. ($^{*}P < 0.05$, $^{**}P < 0.01$, and $^{****}P < 0.0001$, for differences compared with the normal control, and $^{\#}P < 0.05$, $^{\#\#}P < 0.01$, $^{\#\#\#}P < 0.001$, and $^{\#\#\#\#}P < 0.0001$, for differences between animal groups, $n = 6$).

the light-induced RD model.[70,71] In this study, we show that AZD8797 inhibits the gliosis response and rescues the photoreceptors in RD mice. As shown in the behavioral test, severe vision disturbances occur in the RD model. A normal mouse has an exploratory spirit, which would inspire it to go back and forth between the light/dark box to explore.[72,73] After AZD8797 treatment, the behavioral parameters recovered to some extent, indicating that the morphological benefits can be translated successfully into visual improvements.

CX3CL1/CX3CR1 appear to have evolved as a communication means between neurons and microglial cells, being pivotal for preserving tissue homeostasis under normal

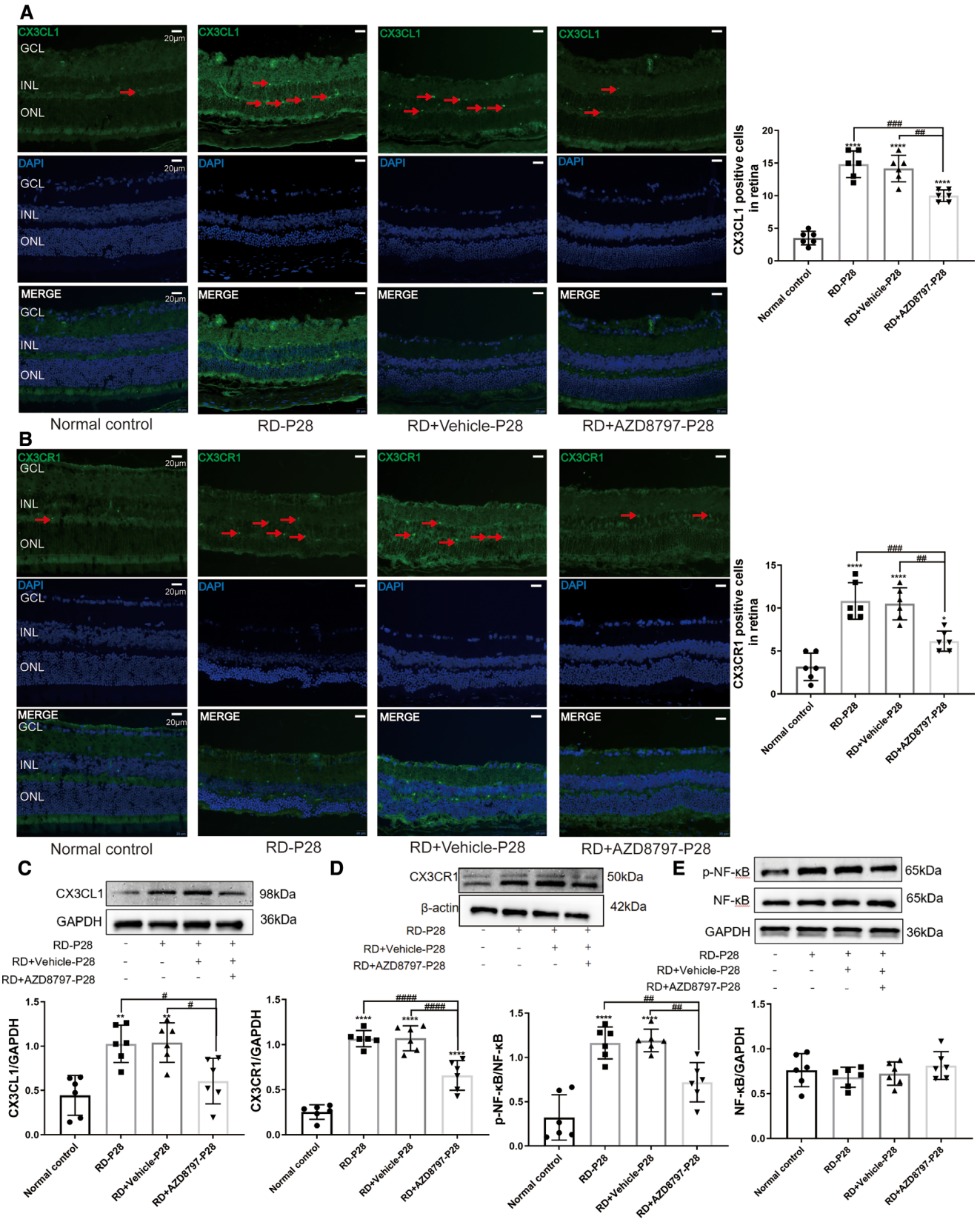

Figure 11. AZD8797 suppress the CX3CL1/CX3CR1 signaling pathway. (**A** and **B**) The number of CX3CL1 and CX3CR1 positive cells in the RD + AZD8797 group, reduced significantly compared with the RD group. (**C**, **D**, and **E**) Western blot results showed that the protein levels of CX3CL1, CX3CR1, and p-NF-κB in the RD + AZD8797 group reduced significantly compared with the RD group, the expression levels of CX3CL, CX3CR1, and NF-κB protein were analyzed by Western blot assay. NF-κB and statistical line chart of gray value. (Scale = 20 μm; $^{*}P < 0.05$, $^{**}P < 0.01$, and $^{****}P < 0.0001$, for differences compared with the normal control, and $^{\#}P < 0.05$, $^{\#\#}P < 0.01$, and $^{\#\#\#}P < 0.001$, for differences between animal groups, $n = 6$).

Investigative Ophthalmology & Visual Science

physiological circumstances.[74] It helps maintain the appropriate distribution of microglia within the retina and also actively regulates continuous microglial "surveying" process.[75] CX3CL1 is expressed in the form of either membrane-bound or secretory ligands in retina. It can modulate the inter-neuron communication and regulate the activation and motility of microglia.[76] The expression level of CX3CL1 can alter dynamically in response to pathological disturbances.[29,77] Elevated CX3CL1 expression has been detected in the retina-choroid tissue of photo-toxicity induced RD model.[78] CX3CL1 is released in the soluble form to induce the microglia migration.[29] Soluble CX3CL1 can further interact with the CX3CR1 in microglia, and facilitate the release of inflammatory factors, including TNF-α, IL-6, and IL-1β.[79] A recent study shows that the severity of photoreceptor death is positively correlated with the CX3CL1/CX3CR1 expressions.[29] In the RD rat model, Müller cells promote the motility of microglia, through upregulating the CX3CL1/CX3CR1 expression in microglial cells.[80] CX3CL1 expression is also strongly induced by classic proinflammatory cytokines, such as TNF-α and IL-1β, IL-4, and interferon-γ (IFN-γ).[81,82] Under pathologic conditions, CX3CL1 staining is most pronounced distributed in the inner nuclear layer (INL), OPL, RPE, and outer limiting membrane (OLM), compared with the fainter staining in the photoreceptor layers.[77] A clinical study also finds that the CX3CR1-positive monocytes accumulate in the retina and subretinal space of patients with RD. These non-classical monocytes will induce neuroinflammation by releasing IL-1β, and exacerbate photoreceptor death.[83,84] A previous study shows that CX3CR1 knockout will cause subretinal microglia activation, accumulation, and photoreceptor death in mouse retina, indicating that physiologic CX3CL1/CX3CR1 signaling is essential for maintaining microglia homeostasis.[85] However, under pathological conditions, the CX3CL1/CX3CR1 signaling can become overactive. The key distinction is that in physiological conditions, CX3CL1 signaling serves a homeostatic and regulatory role, helping to maintain tissue health; whereas in certain pathological conditions, an intriguing phenomenon arises where it can paradoxically promote an inflammatory response. The mechanism of the action of CX3CL1/CX3CR1 signaling pathway in neurological disorders is bidirectional.[86] Chronic levels of retinal inflammation in turn can elevate CX3CL1 levels, in so doing, may influence the vigor of microglial "surveying" behavior and prompt a more rapid dynamic microglial response to insults. For instance, the expressions of CX3CL1 and CX3CR1 are significantly upregulated in the retinas of the RD animal modes, and are obviously downregulated after anti-inflammatory treatment.[87–89] The factors that govern whether a neuroprotective or neurotoxic response occurs likely depend on several variables, including the nature of the initial stimulus, the specific retinal locations, and the localized concentrations of CX3CL1/CX3CR1.[90] Agreed well with aforementioned reports, we find that the CX3CL1/CX3CR1 signaling is activated in the retina of the RD model. These commons indicate that the pharmacological $NaIO_3$ induced mice model can mimic the pathological features of patients with RD to some extent. As a selective antagonist of CX3CR1, AZD8797 can inhibit CX3CR1 binding to the soluble CX3CL1, and mitigates the production of inflammatory cytokine like IL-1β.[79] Moreover, AZD8797 can block the infiltration of CX3CR1-positive leukocytes, and alleviate the brain paralysis.[91] Collectively, these findings suggest that CX3CL1/CX3CR1 signaling is implicated in the pathological mechanism of RD, and CX3CR1 inhibitors, like AZD8797, is effective to ameliorate the retinal inflammation.

NF-κB is a transcription factor that modulates the transcription of inflammatory and immune genes. Notably, NF-κB acts as a downstream mediator factor of CX3CL1/CX3CR1 signaling pathway in RD pathology.[92] NF-κB can also induce the NLRP3 activation and enhance IL-1β production through the HMGB1/caspase-8 pathway.[93] In a rat model of chronic ocular hypertension, transient receptor potential vanilloid 4 (TRPV4) activation induces TNF-α release and exacerbates RGC apoptosis via the JAK2/STAT3/NF-κB pathway in glaucoma.[94] Pan S et al. find that lipopolysaccharide (LPS) enhances the expression of NF-κB and p-p65 in human retinal pigmented epithelial (ARPE-19) cell line, conversely, mitigating the expression of NF-κB will confer benefits on retinal cells.[95] In this context, several pharmacological agents have been used to inhibit the NF-κB signaling in RD models. For instance, erianin, a bibenzyl compound, can suppress the glucose transporter 1-mediated glucose uptake into microglial cells by abrogating the ERK1/2–NF-κB signaling pathway.[96] Moreover, Resvega can inhibit the VEGF-A secretion through and mitigate apoptosis of ARPE-19 cell lines through modulating NF-κB signaling.[97] In this study, we show that CX3CL1/CX3CR1 signaling promotes the release of IL-1β and TNF-α through the phosphorylation of NF-κB. Moreover, AZD8797 can inhibit the phosphorylation of NF-κB, and alleviate the inflammatory response. Accordingly, NF-κB may be developed into a potential therapeutic target for RD.

In summary, this study uncovered a contributory role of CX3CL1/CX3CR1 signaling to the RD pathology. The microglia and Müller cell were activated to induce inflammatory response in the RD mice model. On the other hand, intravitreal injection of AZD8797, a CX3CR1 antagonist, can rescue the photoreceptor, ameliorate the oxidative stress, and inhibit the reactive gliosis. These findings suggest that targeting the neuroglia activation may provide an effective therapeutic strategy for RD.

Acknowledgments

Funded by the National Key Research and Development Program (2018YFA0107303) and the Natural Science Foundation of China (No. 82070990).

Disclosure: **J.-M. Huang**, None; **N. Zhao**, None; **X.-N. Hao**, None; **S.-Y. Li**, None; **D. Wei**, None; **N. Pu**, None; **G.-H. Peng**, None; **Y. Tao**, None

References

1. Wooff Y, Man SM, Aggio-Bruce R, Natoli R, Fernando N. IL-1 family members mediate cell death, inflammation and angiogenesis in retinal degenerative diseases. *Front Immunol*. 2019;10:1618.
2. Goldman D. Müller glial cell reprogramming and retina regeneration. *Nat Rev Neurosci*. 2014;15(7):431–442.
3. Bringmann A, Pannicke T, Grosche J, et al. Müller cells in the healthy and diseased retina. *Prog Retin Eye Res*. 2006;25(4):397–424.
4. Menon M, Mohammadi S, Davila-Velderrain J, et al. Single-cell transcriptomic atlas of the human retina identifies cell types associated with age-related macular degeneration. *Nat Commun*. 2019;10(1):4902.

5. Rathnasamy G, Foulds WS, Ling EA, Kaur C. Retinal microglia - a key player in healthy and diseased retina. *Prog Neurobiol*. 2019;173:18–40.
6. Moriuchi Y, Iwagawa T, Tsuhako A, Koso H, Fujita Y, Watanabe S. RasV12 expression in microglia initiates retinal inflammation and induces photoreceptor degeneration. *Invest Ophthalmol Vis Sci*. 2020;61(13):34.
7. Miller EB, Zhang P, Ching K, Pugh EN, Jr, Burns ME. In vivo imaging reveals transient microglia recruitment and functional recovery of photoreceptor signaling after injury. *Proc Natl Acad Sci USA*. 2019;116(33):16603–16612.
8. Okunuki Y, Mukai R, Pearsall EA, et al. Microglia inhibit photoreceptor cell death and regulate immune cell infiltration in response to retinal detachment. *Proc Natl Acad Sci USA*. 2018;115(27):E6264–E6273.
9. Scholz R, Caramoy A, Bhuckory MB, et al. Targeting translocator protein (18 kDa) (TSPO) dampens pro-inflammatory microglia reactivity in the retina and protects from degeneration. *J Neuroinflammation*. 2015;12:201.
10. Rastogi N, Smith RT. Association of age-related macular degeneration and reticular macular disease with cardiovascular disease. *Surv Ophthalmol*. 2016;61(4):422–433.
11. Nashine S. Potential therapeutic candidates for age-related macular degeneration (AMD). *Cells*. 2021;10(9):2483.
12. Kivinen N. The role of autophagy in age-related macular degeneration. *Acta Ophthalmol*. 2018;96(Suppl A110):1–50.
13. Al-Zamil WM, Yassin SA. Recent developments in age-related macular degeneration: a review. *Clin Interv Aging*. 2017;12:1313–1330.
14. Kaarniranta K, Salminen A, Haapasalo A, Soininen H, Hiltunen M. Age-related macular degeneration (AMD): alzheimer's disease in the eye? *J Alzheimers Dis*. 2011;24(4):615–631.
15. Jarrett SG, Boulton ME. Consequences of oxidative stress in age-related macular degeneration. *Mol Aspects Med*. 2012;33(4):399–417.
16. Boyce M, Xin Y, Chowdhury O, et al. Microglia-neutrophil interactions drive dry AMD-like pathology in a mouse model. *Cells*. 2022;11(22):3535.
17. Handa JT, Bowes Rickman C, Dick AD, et al. A systems biology approach towards understanding and treating non-neovascular age-related macular degeneration. *Nat Commun*. 2019;10(1):3347.
18. Tan W, Zou J, Yoshida S, Jiang B, Zhou Y. The role of inflammation in age-related macular degeneration. *Int J Biol Sci*. 2020;16(15):2989–3001.
19. Taylor AW, Hsu S, Ng TF. The role of retinal pigment epithelial cells in regulation of macrophages/microglial cells in retinal immunobiology. *Front Immunol*. 2021;12:724601.
20. Borst K, Dumas AA, Prinz M. Microglia: immune and non-immune functions. *Immunity*. 2021;54(10):2194–2208.
21. Liddelow SA, Marsh SE, Stevens B. Microglia and astrocytes in disease: dynamic duo or partners in crime? *Trends Immunol*. 2020;41(9):820–835.
22. Ma W, Zhao L, Wong WT. Microglia in the outer retina and their relevance to pathogenesis of age-related macular degeneration. *Adv Exp Med Biol*. 2012;723:37–42.
23. Fu X, Feng S, Qin H, Yan L, Zheng C, Yao K. Microglia: the breakthrough to treat neovascularization and repair blood-retinal barrier in retinopathy. *Front Mol Neurosci*. 2023;16:1100254.
24. Jobling AI, Waugh M, Vessey KA, et al. The role of the microglial Cx3cr1 pathway in the postnatal maturation of retinal photoreceptors. *J Neurosci*. 2018;38(20):4708–4723.
25. Pawelec P, Ziemka-Nalecz M, Sypecka J, Zalewska T. The impact of the CX3CL1/CX3CR1 axis in neurological disorders. *Cells*. 2020;9(10):2277.
26. Fan Q, Gayen M, Singh N. The intracellular domain of CX3CL1 regulates adult neurogenesis and Alzheimer's amyloid pathology. *J Exp Med*. 2019;216(8):1891–1903.
27. Iemmolo M, Ghersi G, Bivona G. The cytokine CX3CL1 and ADAMs/MMPs in concerted cross-talk influencing neurodegenerative diseases. *Int J Mol Sci*. 2023;24(9):8026.
28. Zhang Y, Zhao L, Wang X, et al. Repopulating retinal microglia restore endogenous organization and function under CX3CL1-CX3CR1 regulation. *Sci Adv*. 2018;4(3):eaap8492.
29. Zhang M, Xu G, Liu W, Ni Y, Zhou W. Role of fractalkine/CX3CR1 interaction in light-induced photoreceptor degeneration through regulating retinal microglial activation and migration. *PLoS One*. 2012;7(4):e35446.
30. Cederblad L, Rosengren B, Ryberg E, Hermansson N-O. AZD8797 is an allosteric non-competitive modulator of the human CX3CR1 receptor. *Biochem J*. 2016;473(5):641–649.
31. Ho CY, Lin YT, Chen HH, et al. CX3CR1-microglia mediates neuroinflammation and blood pressure regulation in the nucleus tractus solitarii of fructose-induced hypertensive rats. *J Neuroinflammation*. 2020;17(1):185.
32. Ridderstad Wollberg A, Ericsson-Dahlstrand A, Juréus A, et al. Pharmacological inhibition of the chemokine receptor CX3CR1 attenuates disease in a chronic-relapsing rat model for multiple sclerosis. *Proc Natl Acad Sci USA*. 2014;111(14):5409–5414.
33. Wang J, Iacovelli J, Spencer C, Saint-Geniez M. Direct effect of sodium iodate on neurosensory retina. *Invest Ophthalmol Vis Sci*. 2014;55(3):1941–1953.
34. Machalińska A, Lejkowska R, Duchnik M, et al. Dose-dependent retinal changes following sodium iodate administration: application of spectral-domain optical coherence tomography for monitoring of retinal injury and endogenous regeneration. *Curr Eye Res*. 2014;39(10):1033–1041.
35. Zhao J, Kim HJ, Sparrow JR. Multimodal fundus imaging of sodium iodate-treated mice informs RPE susceptibility and origins of increased fundus autofluorescence. *Invest Ophthalmol Vis Sci*. 2017;58(4):2152–2159.
36. Kakiuchi D, Taketa Y, Ohta E, et al. Combination of circulating microRNAs as indicators of specific targets of retinal toxicity in rats. *Toxicology*. 2019;411:163–171.
37. Palko SI, Saba NJ, Bargagna-Mohan P, Mohan R. Peptidyl arginine deiminase 4 deficiency protects against subretinal fibrosis by inhibiting Müller glial hypercitrullination. *J Neurosci Res*. 2023;101(4):464–479.
38. Telegina DV, Antonenko AK, Fursoa AZ, Kolosova KG. The glutamate/GABA system in the retina of male rats: effects of aging, neurodegeneration, and supplementation with melatonin and antioxidant SkQ1. *Biogerontology*. 2022;23(5):571–585.
39. Tomita H, Sugano E, Fukazawa Y, et al. Visual properties of transgenic rats harboring the channelrhodopsin-2 gene regulated by the thy-1.2 promoter. *PLoS One*. 2009;4(11):e7679.
40. Garcia-Garcia J, Usategui-Martin R, Sanabria MR, Fernandez-Perez E, Telleria JJ, Coco-Martin RM. Pathophysiology of age-related macular degeneration. Implications for treatment. *Ophthalmic Res*. 2022;65(6):615–636.
41. Hageman GS, Luthert PJ, Chong NHV, Johnson LV, Anderson DH, Mullins RF. An integrated hypothesis that considers drusen as biomarkers of immune-mediated processes at the RPE-Bruch's membrane interface in aging and age-related macular degeneration. *Prog Retin Eye Res*. 2001;20(6):705–732.
42. Garcia-Garcia J, Usategui-Martin R, Sanabria MR, Fernandez-Perez E, Telleria JJ, Coco-Martin RM. Pathophysiology of age-related macular degeneration: implications for treatment. *Ophthalmic Res*. 2022;65(6):615–636.

Investigative Ophthalmology & Visual Science

43. Algvere PV, Kvanta A, Seregard S. Drusen maculopathy: a risk factor for visual deterioration. *Acta Ophthalmol*. 2016;94(5):427–433.
44. Ramkumar HL, Zhang J, Chan CC. Retinal ultrastructure of murine models of dry age-related macular degeneration (AMD). *Prog Retin Eye Res*. 2010;29(3):169–190.
45. Enzbrenner A, Zulliger R, Biber J, et al. Sodium iodate-induced degeneration results in local complement changes and inflammatory processes in murine retina. *Int J Mol Sci*. 2021;22(17):9218.
46. Pulukool SK, Bhagavatham SKS, Kannan V, et al. Elevated dimethylarginine, ATP, cytokines, metabolic remodeling involving tryptophan metabolism and potential microglial inflammation characterize primary open angle glaucoma. *Sci Rep*. 2021;11(1):9766.
47. Dheen ST, Kaur C, Ling EA. Microglial activation and its implications in the brain diseases. *Curr Med Chem*. 2007;14(11):1189–1197.
48. Choudhary M, Malek G. A brief discussion on lipid activated nuclear receptors and their potential role in regulating microglia in age-related macular degeneration (AMD). *Adv Exp Med Biol*. 2016;854:45–51.
49. Di Pierdomenico J, García-Ayuso D, Pinilla I, et al. Early events in retinal degeneration caused by rhodopsin mutation or pigment epithelium malfunction: differences and similarities. *Front Neuroanat*. 2017;11:14.
50. Fletcher EL. Contribution of microglia and monocytes to the development and progression of age related macular degeneration. *Ophthalmic Physiol Opt*. 2020;40(2):128–139.
51. Kinuthia UM, Wolf A, Langmann T. Microglia and inflammatory responses in diabetic retinopathy. *Front Immunol*. 2020;11:564077.
52. Alikhan A, Kurek L, Feldman SR. The role of tetracyclines in rosacea. *Am J Clin Dermatol*. 2010;11(2):79–87.
53. Brown EE, Lewin AS, Ash JD. Mitochondria: potential targets for protection in age-related macular degeneration. *Adv Exp Med Biol*. 2018;1074:11–17.
54. Di Pierdomenico J, Scholz R, Valiente-Soriano FJ, et al. Neuroprotective effects of FGF2 and minocycline in two animal models of inherited retinal degeneration. *Invest Ophthalmol Vis Sci*. 2018;59(11):4392–4403.
55. Zhao L, Zabel MK, Wang X, et al. Microglial phagocytosis of living photoreceptors contributes to inherited retinal degeneration. *EMBO Mol Med*. 2015;7(9):1179–1197.
56. Wang M, Wang X, Zhao L, et al. Macroglia-microglia interactions via TSPO signaling regulates microglial activation in the mouse retina. *J Neurosci*. 2014;34(10):3793–3806.
57. Boppana NB, Devarajan A, Gopal K, et al. Blockade of CXCR2 signalling: a potential therapeutic target for preventing neutrophil-mediated inflammatory diseases. *Exp Biol Med (Maywood)*. 2014;239(5):509–518.
58. Muthas D, Reznichenko A, Balendran CA, et al. Neutrophils in ulcerative colitis: a review of selected biomarkers and their potential therapeutic implications. *Scand J Gastroenterol*. 2017;52(2):125–135.
59. Ghosh S, Shang P, Yazdankhah M, et al. Activating the AKT2-nuclear factor-κB-lipocalin-2 axis elicits an inflammatory response in age-related macular degeneration. *J Pathol*. 2017;241(5):583–588.
60. Ghosh S, Padmanabhan A, Vaidya T, et al. Neutrophils homing into the retina trigger pathology in early age-related macular degeneration. *Commun Biol*. 2019;2:348.
61. Wang S, Bai J, Zhang YL, et al. CXCL1-CXCR2 signalling mediates hypertensive retinopathy by inducing macrophage infiltration. *Redox Biol*. 2022;56:102438.
62. Bringmann A, Wiedemann P. Müller glial cells in retinal disease. *Ophthalmologica*. 2012;227(1):1–19.
63. Tackenberg MA, Tucker BA, Swift JS, et al. Müller cell activation, proliferation and migration following laser injury. *Mol Vis*. 2009;15:1886–1896.
64. Joly S, Pernet V, Samardzija M, Grimm C. Pax6-positive Müller glia cells express cell cycle markers but do not proliferate after photoreceptor injury in the mouse retina. *Glia*. 2011;59(7):1033–1046.
65. Linden R, Graca AB, Barber AC, et al. Müller glia activation in response to inherited retinal degeneration is highly varied and disease-specific. *PLoS One*. 2015;10(3):e0120415.
66. Graca AB, Hippert C, Pearson RA. Muller glia reactivity and development of gliosis in response to pathological conditions. *Adv Exp Med Biol*. 2018;1074:303–308.
67. Fernández-Sánchez L, Lax P, Campello L, Pinilla I, Cuenca N. Astrocytes and Müller cell alterations during retinal degeneration in a transgenic rat model of retinitis pigmentosa. *Front Cell Neurosci*. 2015;9:484.
68. Li X, Zhu J, Zhong Y, et al. Targeting long noncoding RNA-AQP4-AS1 for the treatment of retinal neurovascular dysfunction in diabetes mellitus. *EBioMedicine*. 2022;77:103857.
69. Zhao YM, Sun RS, Duan F, et al. Intravitreal slow-release dexamethasone alleviates traumatic proliferative vitreoretinopathy by inhibiting persistent inflammation and Müller cell gliosis in rabbits. *Int J Ophthalmol*. 2023;16(1):22–32.
70. Lu YZ, Fernando N, Natoli R, Madigan M, Valter K. 670nm light treatment following retinal injury modulates Müller cell gliosis: evidence from in vivo and in vitro stress models. *Exp Eye Res*. 2018;169:1–12.
71. Lu YZ, Natoli R, Madigan M, et al. Photobiomodulation with 670 nm light ameliorates Müller cell-mediated activation of microglia and macrophages in retinal degeneration. *Exp Eye Res*. 2017;165:78–89.
72. Suzuki Y, Imayoshi I. Network analysis of exploratory behaviors of mice in a spatial learning and memory task. *PLoS One*. 2017;12(7):e0180789.
73. Storchi R, Rodgers J, Gracey M, et al. Measuring vision using innate behaviours in mice with intact and impaired retina function. *Sci Rep*. 2019;9(1):10396.
74. Lehner C, Spitzer G, Gehwolf R, et al. Tenophages: a novel macrophage-like tendon cell population expressing CX3CL1 and CX3CR1. *Dis Model Mech*. 2019;12(12):dmm041384.
75. Liang KJ, Lee JE, Wang YD, et al. Regulation of dynamic behavior of retinal microglia by CX3CR1 signaling. *Invest Ophthalmol Vis Sci*. 2009;50(9):4444–4451.
76. Arnoux I, Audinat E. Fractalkine signaling and microglia functions in the developing brain. *Neural Plast*. 2015;2015:689404.
77. Silverman MD, Zamora DO, Pan Y, et al. Constitutive and inflammatory mediator-regulated fractalkine expression in human ocular tissues and cultured cells. *Invest Ophthalmol Vis Sci*. 2003;44(4):1608–1615.
78. Chu L, Xiaoxin L, Wenzen Y, et al. Expression of fractalkine (CX3CL1) and its receptor in endotoxin-induced uveitis. *Ophthalmic Res*. 2009;42(3):160–166.
79. Chen G, Zhou Z, Sha W, et al. A novel CX3CR1 inhibitor AZD8797 facilitates early recovery of rat acute spinal cord injury by inhibiting inflammation and apoptosis. *Int J Mol Med*. 2020;45(5):1373–1384.
80. Zhang S, Zhang S, Gong W, et al. Müller cell regulated microglial activation and migration in rats with N-methyl-N-nitrosourea-induced retinal degeneration. *Front Neurosci*. 2018;12:890.
81. Papadopoulos EJ, Sassetti C, Saeki H, et al. Fractalkine, a CX3C chemokine, is expressed by dendritic cells and is up-regulated upon dendritic cell maturation. *Eur J Immunol*. 1999;29(8):2551–2559.

Investigative Ophthalmology & Visual Science

82. Fraticelli P, Sironi M, Bianchi G, et al. Fractalkine (CX3CL1) as an amplification circuit of polarized Th1 responses. *J Clin Invest*. 2001;107(9):1173–1181.
83. Subhi Y, Nielsen MK, Molbech CR, Sørensen TL. Altered proportion of CCR2(+) and CX3CR1(+) circulating monocytes in neovascular age-related macular degeneration and polypoidal choroidal vasculopathy. *Clin Exp Ophthalmol*. 2018;46(6):661–669.
84. Hu SJ, Calippe B, Lavalette S, et al. Upregulation of P2RX7 in Cx3cr1-deficient mononuclear phagocytes leads to increased interleukin-1β secretion and photoreceptor neurodegeneration. *J Neurosci*. 2015;35(18):6987–6996.
85. Zabel MK, Zhao L, Zhang Y, et al. Microglial phagocytosis and activation underlying photoreceptor degeneration is regulated by CX3CL1-CX3CR1 signaling in a mouse model of retinitis pigmentosa. *Glia*. 2016;64(9):1479–1491.
86. Wang X, Xie Y, Niu Y, et al. CX3CL1/CX3CR1 signal mediates M1-type microglia and accelerates high-altitude-induced forgetting. *Front Cell Neurosci*. 2023;17:1189348.
87. Qi Y, Liu L, Liang D, et al. Bujing Yishi tablets alleviate photoreceptor cells death via the P2 × 7R/CX3CL1/CX3CR1 pathway in retinitis pigmentosa rats. *Phytomedicine*. 2023;115:154828.
88. Peng B, Xiao J, Wang K, So KF, Tipoe GL, Lin B. Suppression of microglial activation is neuroprotective in a mouse model of human retinitis pigmentosa. *J Neurosci*. 2014;34(24):8139–8150.
89. Wang K, Peng B, Lin B. Fractalkine receptor regulates microglial neurotoxicity in an experimental mouse glaucoma model. *Glia*. 2014;62(12):1943–1954.
90. Poniatowski ŁA, Wojdasiewicz P, Krawczyk M, et al. Analysis of the role of CX3CL1 (fractalkine) and its receptor CX3CR1 in traumatic brain and spinal cord injury: insight into recent advances in actions of neurochemokine agents. *Mol Neurobiol*. 2017;54(3):2167–2188.
91. Ridderstad Wollberg A, Ericsson-Dahlstrand A, Juréus A, et al. Pharmacological inhibition of the chemokine receptor CX3CR1 attenuates disease in a chronic-relapsing rat model for multiple sclerosis. *Proc Natl Acad Sci USA*. 2014;111(14):5409–5414.
92. Luo P, Chu SF, Zhang Z, Xia CY, Chen NH. Fractalkine/CX3CR1 is involved in the cross-talk between neuron and glia in neurological diseases. *Brain Res Bull*. 2019;146:12–21.
93. Chi W, Chen H, Li F, Zhu Y, Yin W, Zhuo Y. HMGB1 promotes the activation of NLRP3 and caspase-8 inflammasomes via NF-κB pathway in acute glaucoma. *J Neuroinflammation*. 2015;12:137.
94. Li Q, Cheng Y, Zhang S, Sun X, Wu J. TRPV4-induced Müller cell gliosis and TNF-α elevation-mediated retinal ganglion cell apoptosis in glaucomatous rats via JAK2/STAT3/NF-κB pathway. *J Neuroinflammation*. 2021;18(1):271.
95. Pan S, Liu M, Xu H, Chuan J, Yang Z. Lipopolysaccharide activating NF-kB signaling by regulates HTRA1 expression in human retinal pigment epithelial cells. *Molecules*. 2023;28(5):2236.
96. Zhang T, Ouyang H, Mei X, et al. Erianin alleviates diabetic retinopathy by reducing retinal inflammation initiated by microglial cells via inhibiting hyperglycemia-mediated ERK1/2-NF-κB signaling pathway. *FASEB J*. 2019;33(11):11776–11790.
97. Sghaier R, Perus M, Cornebise C, et al. Resvega, a nutraceutical preparation, affects NFκB pathway and prolongs the anti-VEGF effect of bevacizumab in undifferentiated ARPE-19 retina cells. *Int J Mol Sci*. 2022;23(19):11704.

Investigative Ophthalmology & Visual Science